Temperature and Heat Flux in the Delft JHC Burner

SGJ Voorbrood

Department of Multi-Scale Physics, Delft University of Technology

Supervisors: E. Oldenhof & D.J.E.M. Roekaerts

Abstract

In this research, heat fluxes and temperature-properties of the Delft JHC (Jet in Hot Coflow) burner have been measured and calculated using thermocouples and data measured beforehand with LDA and CARS.

The temperature of the outer wall of the JHC burners pipe was measured to be up to 760 K for mixture DJHC-I, containing 16.1 l/min natural gas and 224 l/min air, and 703 K for mixture DJHC-X; 14.2 l/min natural gas and 239 l/min air.The total heat flux leaving the outer wall, mainly (60 %) caused by radiation, was calculated to be 1.3 kJ/s and 1.0 kJ/s for respectively mixture I and X. This is around 20 % of the total energy produced by the combustion of natural gas.

The management of heat fluxes in the system is important, because one wants the operational temperature to be as low as possible, such that combustion products leaving the JHC are relatively clean.

Contents

List of Symbols

Symbol	Description	Unit
A	area, cross-section	m^2
C	constant number	–
c_p	specific heat	$J/g \cdot K$
D, d	thickness, diameter	m
E	energy	J
E	total, hemispherical radiative power per unit area	W/m^2
E_b	total, hemispherical blackbody radiative power per unit area	W/m^2
$E_{b\lambda}$	spectral, hemispherical blackbody radiative power per unit area	W/m^2
E_λ	spectral, hemispherical radiative power per unit area	W/m^2
e	non-chemical energy per unit mass	J/g
F_{i-j}	view factor from i to j	–
Gr	Grashof number	–
g	gravitational constant	m/s^2
$\triangle H_c^0$	heat of combustion at standard conditions	J/m^3
h	sensible (non-chemical) enthalpy per unit mass	J/g
h	sensible enthalpy per mole	J/mol
$\hat{h}$	heat transfer coefficient	$W/m^2 \cdot K$
$I_{b\lambda}$, $I_{b\eta}$	spectral, directional emissive power of a blackbody	W
I_λ, I_η	spectral, directional emissive power	W
i, j	numerators	–
k	thermal conductivity	$W/m \cdot K$
L, l	length	m
M	molar weight	g/mol
m	mass	g
$\dot{m}$	mass flux	g/s
mf	mass fraction	–
n	amount of moles	mol
n	refractive index	–
Nu	Nusselt number	–
p	pressure	bar
P_e	amount of energy converted from chemical to thermal	J/s
Pr	Prandtl number	–
$\dot{Q}$	total heat leaving a system	W
$\dot{q}$	heat flux per unit area	W/m^2
R	universal gas constant	$J/mol \cdot K$
R, r	radius	m
r	radial coordinate	m
Ra	Rayleigh number	–
Re	Reynolds number	–

Symbol	Description	Unit
S	Seebeck coefficient	$\mathrm{V/K}$
s	path length	m
$\hat{s}$	unit vector	–
T	temperature	K, °C
U	potential difference	V
v	velocity	$\mathrm{m/s}$
$\dot{W}$	work done to a system	W
x, y, z	Carthesian coordinates	m
Y, y	mole fraction	–
α	thermal diffusivity	$\mathrm{m^2/s}$
β	bulk expansion coefficient	$\mathrm{1/K}$
$\triangle_1^2$	difference prefix $(_2-_1)$	–
ϵ	total, hemispherical emissivity	–
ϵ_λ	spectral, hemispherical emissivity	–
ϵ'_λ	spectral, directional emissivity	–
ϑ	angle coordinate	–
κ_η	linear absorption coefficient	$\mathrm{1/m}$
μ	dynamic viscosity	$\mathrm{g/m{\cdot}s}$
ν	kinematic viscosity	$\mathrm{m^2/s}$
ρ	density	$\mathrm{g/m^3}$
ρ^0	density at standard conditions	$\mathrm{g/m^3}$
σ	Stefan-Boltzmann constant	$\mathrm{W/m^2{\cdot}K}$
τ_η	optical thickness	–
ϕ_m	mass flux	$\mathrm{g/s}$
ϕ_q	heat leaving a system	$\mathrm{J/s}$
ϕ_V	volume flux	$\mathrm{m^3/s}$
ϕ_w	work done to a system	$\mathrm{J/s}$
ψ	azimuthal angle coordinate	–
Ω	solid angle	–

Chapter 1

Introduction

The Delft Jet in Hot Coflow Burner was built for investigations on mild combustion. In a furnace, mild combustion takes place when mixing combustion products with the ingoing airstream, thus preheating this flow, but also diluting it, such that the auto-ignition limit is reached. It is understood that mild combustion happens at a very uniform temperature, is fuel efficient and reduces the NO_x-emissions (which increase with the combustion temperature).

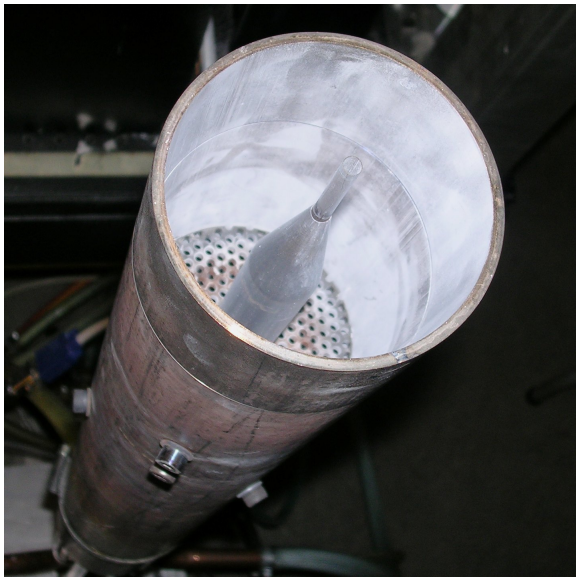

Figure 1.1: Top view of the Delft JHC Burner

In the Delft JHC Burner this situation is modelled. Natural gas combusts by mixing it with a hot coflow of hot and diluted air, generated by a secondary burner inside an annulus, at the bottom of a pipe. The coflow loses part of its

heat to the surroundings by radiative and convective heat transfer at the outside of the pipe. As seen in figure 1.2, the mild combustion occurs at the higher end of the pipe, where the hot coflow mixes with the primary fuel. This happens at a relatively low temperature, therefore the flame is hardly visible. The burner allows the experimentator to control oxygen content, velocity and temperature of the hot coflow. (this last option is obtained by cooling with pressurized air in the central duct)

Furthermore, the flame properties in the primary burner depend highly on the composition of the coflow.

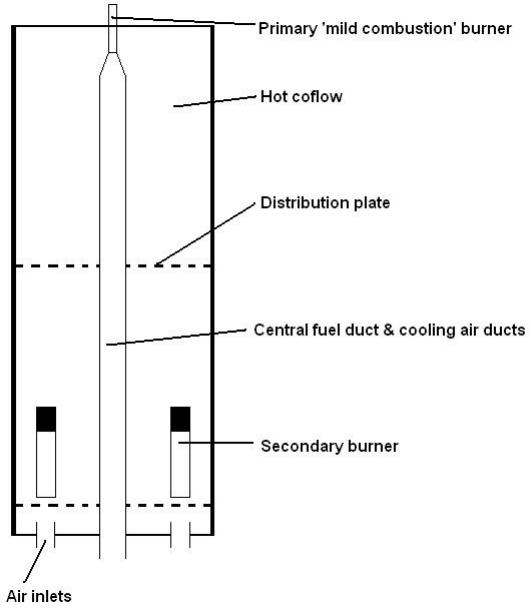

Figure 1.2: A simple scheme of the Delft JHC Burner, showing the placement of the two burners and the inner pipe within the system.

To be able to optimize the Delft JHC Burner, it is very important that more insight in the heat fluxes is gained.

Because of the high temperatures, it is expected that radiative heat transfer at the outer tube plays an important role. Calculations and measurements in this research will give the heat fluxes taking place in the Delft JHC Burner.

Also, to find an estimation of the composition of the coflow, calculations on the secondary burner will be done in this research.

Chapter 2

Theoretical Background

2.1 Energy balance

To get insight in the thermal behaviour inside the burner, balances are necessary. Because the main target is to unravel the thermodynamic properties of the primary burner and hot coflow, we focus on the part of the pipe between the secondary and primary burner (see figure 1.2). The energy balance over the volume of the pipe states:

$$\frac{dE}{dt} = \phi_{m,in} \cdot e_{in} - \phi_{m,out} \cdot e_{out} - \phi_q + \phi_w + P_e = 0 \tag{2.1}$$

Where $\phi_m = \frac{dm}{dt} = \dot{m}$ are the total mass-fluxes entering and leaving the system, P_e is the energy production per second, $\phi_w = \frac{dW}{dt} = \dot{W}$ the work done per second by the outside to the control-volume and $\phi_q = \frac{dQ}{dt} = \dot{Q}$ the energy leaving the system as heat.

Furthermore, the energy production can be calculated by

$$P_e = \Delta H_c^0 \cdot \phi_{V,gas} \tag{2.2}$$

with ΔH_c^0 the heat of combustion of natural gas in $^{\mathrm{J}}/_{\mathrm{m}^3}$ at standard conditions ($T = 0\,^{\circ}\mathrm{C}$, $p = 1\,\mathrm{atm}$).

In equation 2.1, e is the mass-concentration of total non-chemical energy; the sum of the enthalpy per unit mass h, potential energy per unit mass and kinetical energy per unit mass:

$$e = h + g \cdot z + \frac{1}{2} \cdot v^2 \tag{2.3}$$

with $g = 9.81\,^{\mathrm{m}}/_{\mathrm{s}^2}$ the earth's gravitational acceleration, velocity v and z the relative height.

The enthalpy h that will be used in the research is the so called 'sensible enthalpy'; the integral of the specific heat c_p

$$h = \int_{T_0}^{T} c_p \cdot dT \tag{2.4}$$

For convenience a difference in mass-concentration of energy $\Delta e = \Delta_1^2 e = e_2 - e_1$ will be used

$$\Delta e = \Delta h + g \cdot \Delta z + \frac{1}{2}\Delta\left(v^2\right) \tag{2.5}$$

2.1.1 Thermodynamic properties of an ideal gas mixture

Because the gas that will be analyzed is a complex mixture of diverse components, properties such as the enthalpy cannot be taken from existing tables. To find the enthalpy $h\left(p,T\right)$, the mole fraction y_i of each component i needs to be known, as well as the enthalpy $h_i\left(T\right)$ of each of the components.

When analysing a mixture of total mass m, consisting of j components with a mass m_i and a molecular weight M_i, we first find the amount of moles n_i of the components

$$n_i = \frac{m_i}{M_i} \tag{2.6}$$

which gives the total number of moles in the mixture n when summed

$$n = \sum_{i=1}^{j} n_i = \sum_{i=1}^{j} \frac{m_i}{M_i} \tag{2.7}$$

Next, the mole fraction of each compoment can be found by

$$y_i = \frac{n_i}{n} \tag{2.8}$$

Now the molar enthalpy of the mixture $\bar{h}$ can be calculated by a weighed summation of $\bar{h_i}$, the molar enthalpy of each component, as

$$\bar{h} = \sum_{i=1}^{j} y_i \cdot \bar{h_i} \tag{2.9}$$

The enthalpy of the components is temperature dependent and can be looked up in tables. It is related to the molar enthalpy by

$$\overline{h} = M \cdot h \tag{2.10}$$

$$\overline{h_i} = M_i \cdot h_i \tag{2.11}$$

where the molecular weight M of the mixture is the mole-fraction average of the component molecular weights:

$$M = \sum_{i=1}^{j} y_i \cdot M_i \tag{2.12}$$

2.1.2 Averaging thermodynamic properties

We introduce the notation $\langle\rangle$ to denote a cross-sectional mass-average.

Then, the mass-flux appearing in formula 2.1 can be written as a function of the volume-flux ϕ_V by

$$\phi_m = \langle\rho\rangle \cdot \phi_V \tag{2.13}$$

and as a function of the average velocity $\langle v\rangle$ by

$$\phi_m = A \cdot \langle\rho\rangle \cdot \langle v\rangle \tag{2.14}$$

Later on, we will use the (mass-)average values of velocity $\langle v\rangle$ and enthalpy $\langle h\rangle$. To calculate these, we rewrite equation 2.14, where ρ is now a function of the position (here r, because we assume cylindrical symmetry):

$$\phi_m = A \cdot \langle\rho\rangle \cdot \langle v\rangle = \int_{r_1}^{r_2} 2\pi \cdot r \cdot \rho\left(r\right) \cdot v\left(r\right) \cdot dr \tag{2.15}$$

Removing the non-r-dependent factors 2π from the integrals yields the mass-averaged velocity :

$$\langle v\rangle = \frac{\int_{r_1}^{r_2} r \cdot \rho \cdot v \cdot dr}{\int_{r_1}^{r_2} r \cdot \rho \cdot dr} \tag{2.16}$$

For the enthalpy we can use a similar method. We state the following notation for the total heat flux through a cylinder:

$$\dot{Q} = \int_{r_1}^{r_2} 2\pi \cdot r \cdot \rho\left(r\right) \cdot v\left(r\right) \cdot h\left(r\right) \cdot dr \equiv \langle h\rangle \cdot \phi_m \tag{2.17}$$

Combining this with formula 2.15, and once again removing unnecessary factors, gives rise to the mass-averaged enthalpy $\langle h\rangle$:

$$\langle h\rangle = \frac{\int_{r_1}^{r_2} r \cdot \rho \cdot v \cdot h \cdot dr}{\int_{r_1}^{r_2} r \cdot \rho \cdot v \cdot dr} \tag{2.18}$$

2.2 Heat transfer

To be able to calculate the heat $\dot{Q}$ leaving the system, different types of heat fluxes need to be considered.

In the walls of the outer and inner tubes conduction takes place. Between the tubes and from the outside of the outer tube to the surroundings of the pipe there is radiation. A third type of heat flux is the convection at for example the outer wall of the pipe.

Heatflux and temperature difference are usually related by Newtons Law of Cooling:

$$\dot{Q} = \widehat{h} \cdot A \cdot \Delta T \tag{2.19}$$

Where A represents the area of the surface, ΔT the difference in temperature and $\widehat{h}$ the heat transfer coefficient in $^{\mathrm{W}}/_{\mathrm{m}^2 \cdot \mathrm{K}}$.

Very commonly in heat transfer, the unitless *Nusselt number* (Nu) is used to express the heat transfer coefficient in terms of the thermal conductivity k, which is a material property. The Nusselt number can be described as the ratio of total heat transfer to the conductive heat transfer in a plane geometry.

$$Nu = \frac{\widehat{h} \cdot D}{k} \tag{2.20}$$

In formula 2.20 D represents the characterisitic length scale. Typically, the *Nusselt number* is expressed as a function of a variety of other unitless numbers (like the *Prandtl, Grashof* and *Reynolds number*s), often found empirically.

2.2.1 Conduction

Thermal conduction is a type of molecular transport that gives rise to a heatflux within a material when a temperature gradient ∇T is present. The heatflux vector per unit area $\overrightarrow{\dot{q}}$ is given in vector notation as:

$$\overrightarrow{\dot{q}} = -k \nabla T \tag{2.21}$$

For a uniform temperaturegradient only nonzero in the x-direction and a constant k this becomes:

$$\dot{q} = -k \cdot \frac{dT}{dx} \tag{2.22}$$

with k the thermal conductivity in $^{\mathrm{W}}/_{\mathrm{m} \cdot \mathrm{K}}$. In a steady state, the heatflux is constant, and integrating formula 2.22 to x over a wall-thickness D gives the relation between heatflux and temperature-difference ΔT as

$$\dot{q} = -\frac{k}{D} \cdot \Delta T \tag{2.23}$$

Obviously, for this case $\widehat{h} = \frac{k}{D}$, or more shortly: $Nu = 1$.

Now, because of the cilindrical geometry this will not hold for the burner pipe. The total heatflux is still constant, but the area A depends on the radius r.

$$\dot{Q} = A \cdot \dot{q} = 2\pi r L \cdot \dot{q} \tag{2.24}$$

Combining equations 2.21 and 2.24 and considering a cylindrical symmetry with just a temperature gradient in the r-direction leads to:

$$-k \cdot \frac{dT}{dr} = \frac{C_1}{2\pi r L} \tag{2.25}$$

$$T(r) = -\frac{C_1}{2\pi L k} \ln(r) + C_2 \tag{2.26}$$

by integration to r with C_1 and C_2 constants.

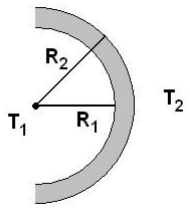

Figure 2.1: A cilinder with inner and outer radii R_1 and R_2 and temperatures T_1 and T_2.

Using figure 2.1 and the relations $T(R_1) = T_1$ and $T(R_2) = T_2$ the temperatureprofile in a cilinder is found:

$$\frac{T(r) - T_2}{T_1 - T_2} = \frac{\ln({}^{r}/_{R_2})}{\ln({}^{R_1}/_{R_2})} \tag{2.27}$$

$$\frac{dT}{dr} = \frac{(T_1 - T_2)}{\ln({}^{R_1}/_{R_2})} \cdot \frac{1}{r} \tag{2.28}$$

Applying this equation into 2.21 gives the heatflux in the wall of a steady-state cilinder

$$\dot{q} = -\frac{k}{R_2 \cdot \ln({}^{R_1}/_{R_2})} \cdot \Delta T = -\frac{2k}{D_2 \cdot \ln({}^{R_1}/_{R_2})} \cdot \Delta T \tag{2.29}$$

2.2.2 Radiation

All materials emit radiation in the form of photons, covering the entire electromagnetic spectrum. The spectral, directional emissivity $\epsilon_{\lambda}^{'}$ compares the actual spectral, directional emissive power I_{λ} with that of a black surface $I_{b\lambda}$ (which is equal for all directions)

$$\epsilon_{\lambda}^{'}(T,\lambda,\hat{s}) = \frac{I_{\lambda}(T,\lambda,\hat{s})}{I_{b\lambda}(T,\lambda)} \tag{2.30}$$

Often, instead of I_{λ}, I_{η} is used.

The spectral, hemispherical emissivity is found by integrating the directional emissive powers over all directions $\hat{s}$ and defined by [2] as

$$\epsilon_{\lambda}(T,\lambda) = \frac{E_{\lambda}(T,\lambda)}{E_{b\lambda}(T,\lambda)} \tag{2.31}$$

where

$$E_{\lambda}(T,\overrightarrow{r}) = \int_0^{2\pi}\int_0^{\pi/2} I_{\lambda}(T,\overrightarrow{r},\vartheta,\psi)\cos(\vartheta)\sin(\vartheta)\,d\vartheta d\psi \tag{2.32}$$

and because of the diffusive property of a blackbody

$$E_{b\lambda}(T,\lambda) = I_{b\lambda}(T,\lambda)\cdot\int_0^{2\pi}\int_0^{\pi/2}\cos(\vartheta)\sin(\vartheta)\,d\vartheta d\psi = \pi\cdot I_{b\lambda}(T,\lambda) \tag{2.33}$$

This leads to

$$\epsilon_{\lambda}(T,\lambda) = \frac{1}{\pi}\int_0^{2\pi}\int_0^{\pi/2}\epsilon_{\lambda}^{'}(T,\lambda,\hat{s})\cos(\vartheta)\sin(\vartheta)\,d\vartheta d\psi \tag{2.34}$$

When we consider the source to be diffusive, $\epsilon_{\lambda}^{'}$ does not depend on direction, and we find, according to [2],

$$\epsilon_{\lambda}^{'}(T,\lambda,\hat{s}) = \epsilon_{\lambda}(T,\lambda) \tag{2.35}$$

The total, hemispherical emissivity ϵ or simply emissivity, can be found by integrating over the whole spectrume and is defined as

$$\epsilon(T) = \frac{E(T)}{E_b(T)} \tag{2.36}$$

with $E(T)$ and $E_b(T)$ being respectively the total hemispherical power and the total blackbody power per unit area (in $\mathrm{W/m^2}$), formulated as

$$E(T) = \int_0^\infty E_\lambda(T, \lambda)\, d\lambda \tag{2.37}$$

When an object is not only diffuse, but also gray, the emissivity does not depend on wavelength either, so

$$\epsilon_\lambda(T, \lambda) = \epsilon(T) \tag{2.38}$$

By use of the well known formula for total emissive power of a blackbody

$$E_b(T) = n^2 \varepsilon \sigma T^4 \tag{2.39}$$

the total hemispherical radiation $\dot{q}_r$ for a gray-diffuse body in $\mathrm{W/m^2}$ can be formulated as

$$\dot{q}_r = E(T) = \epsilon \cdot E_b(T) = \varepsilon \sigma T^4 \tag{2.40}$$

with $\sigma = 5.670 \cdot 10^{-8} \mathrm{W/m^2K^4}$ the Stefan-Boltzmann constant and n the refractive index. $n \simeq 1$ for ordinary gases.

2.2.2.1 View Factors

To express the fraction of radiosity leaving a surface (i) that arrives at another surface (j) view factors are used. The view factor F_{i-j} is dependent only of the geometry of the unit, and therefore for each geometry related view factors have to be calculated.

Logically, the sum of all view factors is 1. Furthermore, the reciprocity rule for view factors states

$$F_{i-j} = F_{j-i} \tag{2.41}$$

For a cylinder within a cylinder, the view factor from the interior of the outer cylinder to itself is given by

$$F_{2-2} = 1 - \frac{1}{R^*} + \frac{2}{\pi R^*} \cdot \arctan\left(\frac{2\left(R^{*2}-1\right)^{1/2}}{l^*}\right) - \frac{l^*}{2\pi R^*} \cdot \ldots$$

$$\ldots \left\{ \frac{\left(4R^{*2}+l^{*2}\right)^{1/2}}{l^*} \cdot \arcsin\left(\frac{4\left(R^{*2}-1\right)+\left(l^{*2}/R^{*2}\right)\left(R^{*2}-2\right)}{l^{*2}+4\left(R^{*2}-1\right)} \right) - \arcsin\left(\frac{R^{*2}-2}{R^{*2}}\right) + \frac{\pi}{2}\left[\frac{\left(4R^{*2}+l^{*2}\right)^{1/2}}{l^*} - 1 \right] \right\} \tag{2.42}$$

and the view factor from the interior of the outer cylinder to the inner cylinder by

$$F_{2-1} = \frac{1}{R^*} - \frac{1}{\pi R^*} \cdot \left\{ \arccos\left(\frac{b}{a}\right) - \frac{1}{2l^*}\left[(a+2)^2 - (2R^*)^2\right]^{1/2} \cdot \arccos\left(\frac{b}{aR^*}\right) + b \cdot \arcsin\left(\frac{1}{R^*}\right) - \frac{a}{2} \right\} \tag{2.43}$$

with $R^* = \frac{R_2}{R_1}$, $l^* = \frac{l}{R_1}$, $a = l^{*2} + R^{*2} - 1$ and $b = l^{*2} - R^{*2} + 1$ (from [4])

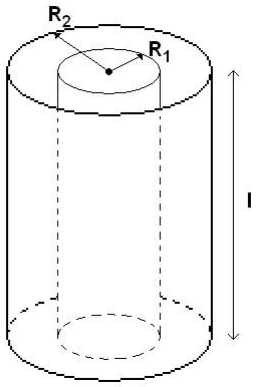

Figure 2.2: A cylinder with radius R_1 within a big cylinder (radius R_2), both with length l.

2.2.2.2 Radiation in participating media

If we assume the participating medium (in this case, the coflow), to be non-scattering, we find the source function I_η with path length s to be

$$I_\eta(\tau_\eta) = I_\eta(0) \cdot e^{-\tau_\eta} + \int_0^{\tau_\eta} I_{b\eta}(\tau'_\eta) \cdot e^{-(\tau_\eta - \tau'_\eta)} \cdot d\tau'_\eta \tag{2.44}$$

with $\tau_\eta = \int_0^s \kappa_\eta \cdot ds$ the optical thickness, k_η the linear absorption coefficient, $I_{b\eta}(0)$ the blackbody intensity at location s', and $I_\eta(0)$ the initial intensity (so $s = 0$), without absorbing/emitting.

So, the first part of function 2.44 is the attenuation of the original, directional intensity by the coflow. The second part is the addition of energy by emission of the hot coflow, in the same direction.

Integrating over all wavelengths, directions, and surface areas then gives the amount of energy arriving at a surface. The amount of energy arriving (or leaving) at a little volume element in the coflow is found by making a balance of emission and absorption.

Unfortunately, for a complex case such as the coflow in the DJHC, the heat fluxes can only be found if the temperature field is known, and vice versa. Numerical methods are needed to solve the problem.

2.2.3 Natural Convection

When a surface, surrounded by a fluidum, is hot, it will heat up the fluidum by conduction, lowering its density. This causes the fluidum to move and allows colder fluidum to take its place, hereby speeding up the heat transfer. This is

called free or natural convection, and is sometimes referred to as thermobuoyant flow.

The most convenient way to calculate the heat transferred by natural convection in the system described is by use of a *Nusselt number* (equation 2.20). The *Nusselt number* for the natural convection of a vertical cylinder is given by [6]

$$Nu_x = \left[Nu_0 + Gr_L^{\frac{1}{6}} \cdot Pr^{\frac{1}{6}} \cdot \left(\frac{f_4}{300} \right) \right]^2 \tag{2.45}$$

with $Nu_0 = 0.68$ for a vertical cylinder and

$$f_4 = \left[1 + \left(\frac{0.5}{Pr} \right)^{\frac{9}{16}} \right]^{\frac{-16}{9}} \tag{2.46}$$

Another way to calculate the *Nusselt number* for a vertical cylinder is given by [4] (but only holds when $\frac{2r}{L} \gtrsim \frac{35}{Gr_L^{\frac{1}{4}}}$)

$$Nu_L = \left[Nu_{L,l}^6 + Nu_{L,t}^6 \right]^{\frac{1}{6}} \tag{2.47}$$

where $Nu_{L,l}$ and $Nu_{L,t}$ are the laminar and turbulent parts:

$$Nu_{L,l} = \frac{2.8}{\ln\left[1 + {}^{2.8}/_{\left(a_1 Ra_L^{\frac{1}{4}} \right)} \right]} \tag{2.48}$$

$$Nu_{L,t} = \frac{0.13 Pr^{0.22}}{\left(1 + 0.61 Pr^{0.81} \right)^{0.42}} \cdot Ra_L^{\frac{1}{3}} \tag{2.49}$$

with a_1 being

$$a_1 = \frac{4}{3} \cdot \frac{0.503}{\left[1 + \left({}^{0.492}/_{Pr} \right)^{\frac{9}{16}} \right]^{\frac{4}{9}}} \tag{2.50}$$

In these formulas Gr, Pr and Ra represent the *Grashof, Prandtl* and *Rayleigh numbers* respectively. These three unitless numbers are used to describe the ratio of buoyancy forces to viscous forces (Gr), the ratio of kinematic viscosity versus the thermal diffusivity (Pr) and the presence of buoyancy driven flow (Ra) and are calculated as

$$Gr_L = \frac{g \beta \Delta T}{\nu^2} \cdot L^3 \tag{2.51}$$

$$Pr = \frac{\nu}{\alpha} \tag{2.52}$$

$$Ra_L = Gr_L \cdot Pr = \frac{g \beta \Delta T}{\nu \cdot \alpha} \cdot L^3 \tag{2.53}$$

Here x is the position parameter, ν is the kinematic viscosity of the fluid in $^{m^2}/_{s}$, β the bulk expansion coefficient of the fluid in $^{1}/_{K}$, L the characteristic length scale, g the gravitational acceleration and α the thermal diffusivity of the fluid in $^{m^2}/_{s}$.

Note the presence of indices $_x$ and $_L$; when the first is used, the unitless number is local at position x and thus position-dependent. When the second is used, the number is the average over a surface of length L.

The thermal diffusivity can be computed by

$$\alpha = \frac{k}{\rho \cdot c_p} \tag{2.54}$$

For ideal gases the thermal expansion is

$$\beta = \frac{1}{T} \tag{2.55}$$

2.2.4 Driven convection

Heat transfer by forced or driven convection is similar to free convection, except that now the fluid motion is mostly generated by an external source instead of thermobuoyancy.

When analyzing driven convection, another unitless quantity, the *Reynolds number* is needed in the calculation for the *Nusselt number*. The *Reynolds number* Re is the ratio between inertial and viscous forces and is equal to

$$Re = \frac{d \cdot \langle v \rangle}{\nu} = \frac{\rho \cdot \langle v \rangle \cdot d}{\mu} \tag{2.56}$$

Where $\langle v \rangle$ is the average velocity of the fluid, μ is the dynamic viscosity in $Pa \cdot s = {}^{kg}/_{m \cdot s}$ and ρ the density.

For circular cylinders, the *Nusselt numbers* for the convection caused by a fully developed flow are

- For laminar flows ($Re \leq 2,300$) [4, 3]

$$\langle Nu \rangle = 3.66 \tag{2.57}$$

- For turbulent flows ($Re \gtrsim 10^4$) [3]

$$\langle Nu \rangle = 0.027 Re^{0.8} \cdot Pr^{0.33} \tag{2.58}$$

  Or, with $n = 0.3$ for outward heatflux, $n = 0.4$ for inward heatflux, [4]

$$\langle Nu \rangle = 0.023 Re^{0.8} \cdot Pr^{n} \tag{2.59}$$

- For transitional flows ($2,300 < Re < 10^4$) [4]

$$\langle Nu \rangle^{10} = \langle Nu_l \rangle^{10} + \left(\frac{\exp^{(2,200 - Re)/365}}{\langle Nu_l \rangle^2} + \frac{1}{\langle Nu_t \rangle^2} \right)^{-5} \tag{2.60}$$

with d the characteristic length scale: the diameter of the tube.

Next, the *Nusselt numbers* for the heat flux caused by a laminar, fully developed flow in an annulus (outer diameter D_1) to the inner surface (diameter D_2) are listed in table 2.1 [4]

D_1/D_2	$\langle Nu \rangle$
0.05	17.81
0.10	11.91
0.20	8.499
0.40	6.583
0.60	5.912
0.80	5.580
1.00	5.385

Table 2.1: Nusselt numbers for a laminar fully developed flow in an annulus for some ratio between inner diameter D_2 and outer diameter D_1.

For the calculation of the Nusselt number describing the heat flux at the outer wall, considering a turbulent and transitional flows in an annulus, the same formulae for can be used as for circular cylinders (2.58, 2.59 and 2.60).

2.3 Thermocouples

In order to measure temperatures over a relatively wide range, thermocouples can be used. A thermocouple is constructed by connecting two different types of conductors (usually in form of a wire).

The thermoelectric or Seebeck effect states that in any conductor exposed to a thermal gradient a potential difference arises. This potential difference U_a in a wire is calculated by

$$U_a = S_a \cdot (T_1 - T_2) \tag{2.61}$$

with S_a the Seebeck coefficient. [5]

When this conductor a is connected with another type of conductor b, with a different Seebeck coefficient S_b, a net voltage U_{ab} is created if $T_1 \neq T_2$ by

$$U_{ab} = U_a - U_b = (S_a - S_b) \cdot (T_1 - T_2) = S_{ab} \cdot (T_1 - T_2) \tag{2.62}$$

The values of the sensitivity S_{ab} for some of the most common thermocouple types are listed in table 2.2, together with the temperature range in which they can be used.

Type	S_{ab} (μV/K)	Temperature range (°C)	Composition
T	43	-250 to +400	copper-constantan
J	50	-180 to +800	iron-constantan
E	68	-40 to +900	chromel-constantan
K	41	-180 to +1300	chromel-alumel
B,R,S	10	-50 to +1800	different platinum/rhodium alloys
N	39	-270 to +1300	nicrosil-nisil

Table 2.2: Some thermocouple types with their sensitivity S_{ab}, temperature range and composition.

Unfortunately, in reality the sensitivity is not linear (although close to), but it can be approximated by a polynomial or looked up in tables corresponding with the thermocouple type.

Chapter 3

Experimental Setup

3.1 Description of the Delft JHC Burner

Before rushing to find the unknowns to be solved and the data to be measured, let's give a more precise description of the Delft Jet-in-Hot-Coflow burner first.

In the center of the Delft JHC Burner is a fuel duct, transporting natural gas upward. Around this fuel duct is another double duct, containing the cooling airflow. This air goes upward directly around the fuel duct and back downward in the surrounding cylinder, as can be seen in figure 3.1, effectively keeping the fuel cool. [7]

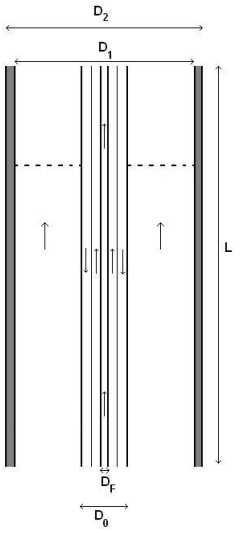

Figure 3.1: Schematic figure of the Delft JHC Burner with some of the lengths.

Around the central duct (meaning the total fuel and cooling system) the hot coflow is flowing. As explained before, this hot coflow is confined by the outer tube. A distribution plate is placed just above the secondary burners, so that the temperature of the hot coflow can be presumed uniform. At the upper end of the tube, the hot coflow mixes with the fuel leaving the fuel duct, causing combustion. The control volume does not cover this combustion.

In the following table, some of the length-scales are given, together with their values for the Delft JHC Burner. [7, 8]

Name	Value	Explanation
D_F	4.25 mm	Diameter of the fuel duct
D_0	22.0 mm	Outer diameter of the inner tube
D_1	82.5 mm	Inner diameter of the outer tube
D_2	88.9 mm	Outer diameter of the outer tube
L	600 mm	Length of the cylinder

Table 3.1: Some length-scales of the Delft JHC Burner

3.2 Energy balances for the Delft JHC Burner

Next it is necessary to specificy the energy balance for the JHC Burner.

No work is done to the control-volume, thus in formula 2.1, $\dot{W} = 0$

Also, because the problem is steady-state, we have $\phi_m = \phi_{m,in} = \phi_{m,out}$

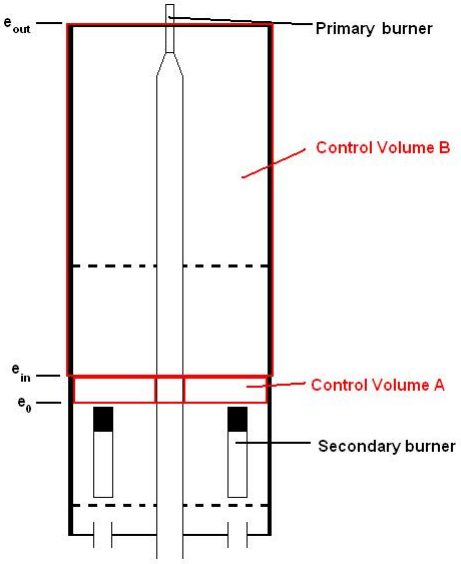

Figure 3.2: A simple scheme of the Delft JHC Burner, showing the position of the twoControl Volumes.

Now, looking at figure 3.2, the more specific energy balance is found for the small region of the secondary burner, Control Volume A (where we neglect heatfluxes, thus $\dot{Q} = 0$)

$$P_e = \phi_m \cdot \Delta e_1 = \phi_m \cdot \Delta_0^{in} e \tag{3.1}$$

where e_0 is the energy concentration of the coflow just before the secondary burner, and e_{in} is the energy concentration of the coflow just after combustion. Hence P_e can be described as the heat converted from chemical to thermal by combustion.

In the region from the secondary burner to the end of the tube (figure 3.2), there is only a loss of energy of the coflow by heat leaving the system, leading to Control Volume B

$$\dot{Q} = \phi_m \cdot \Delta e_2 = \phi_m \cdot \Delta^{in}_{out} e \tag{3.2}$$

Here e_{out} is the concentration of energy of the coflow when leaving the tube.

The heat $\dot{Q}$ leaving the system is the sum of heat fluxes from the outer tube, and the inside, containing the cooling duct and the fuel duct.

$$\dot{Q} = \dot{Q}_{wall} + \dot{Q}_{cool} \tag{3.3}$$

3.3 Control Volume A

3.3.1 Composition of the coflow

First of all, we use the (molar) compositions Y of air [11] and natural gas [6] as can be found in table 3.2.

Air	Y (%)
Nitrogen	78.084
Oxygen	20.946
Argon	0.934
Carbon Dioxide	0.038

Natural 'Groningen' Gas	Y (%)
Methane	81.29
Nitrogen	14.32
Ethane	2.87
Carbon Dioxide	0.89
Propane	0.38
Butane	0.15
Hexane	0.05
Pentane	0.04
Oxygen	0.01

Table 3.2: Composition of dry air and dutch natural gas in molar percents Y.

We assume perfect combustion; all alkanes in the natural gas react complete with oxygen from the air to water and carbon dioxide. As a result, the coflow will be a mixture of oxygen, argon, nitrogen, carbon dioxide and water.

The massflow of the gas $\phi_{m,gas}$ and the massflow of air $\phi_{m,gas}$ can now be used with their respective compositions to find the exact mixture of the coflow after ideal combustion. The massflow of the coflow ϕ_m equals

$$\phi_m = \phi_{m,gas} + \phi_{m,air} \tag{3.4}$$

In this experiment we consider two cases, DJHC-I and DJHC-X, with two different gas and air massflows. Because only a volumeflow is given, we need to transform the data into molar and mass fractions (as explained in subsection 2.1.1) to find the coflow properties for both cases. To do this, we will need their densities. From literature[3] we find $\rho_{air} = 1.293\,\mathrm{kg/m^3}$ and $\rho_{gas} = 0.833\,\mathrm{kg/m^3}$ at $T = 0\,^\circ\mathrm{C}$. These can be converted to densities at room temperature $T = 23.5\,^\circ\mathrm{C}$ by the ideal gas model: $T_1 \cdot \rho(T_1) = T_2 \cdot \rho(T_2)$

The volume- and massflows of air and natural gas for DJHC-I and DJHC-X, as well as the resulting coflow compositions are given in table 3.3. For more complete data we refer to Appendix A.

DJHC-I	ϕ_V (nL/min)	ϕ_m (g/s)
Air	224.0	4.415
Natural Gas	16.10	0.2044

Coflow I	Y (%)
Nitrogen	73.69
Water	11.67
Oxygen	7.69
Carbon Dioxide	6.08
Argon	0.87

DJHC-X	ϕ_V (nL/min)	ϕ_m (g/s)
Air	239.0	4.711
Natural Gas	14.20	0.1803

Coflow X	Y (%)
Nitrogen	74.41
Water	9.76
Oxygen	9.86
Carbon Dioxide	5.09
Argon	0.88

Table 3.3: Initial volume- and massflows ϕ_V and ϕ_m of air and gas and the resulting composition of the coflow for case DJHC-I and DJHC-X.

The massflow of the coflow is found without difficulties, using equation 3.4. For DJHC-I and DJHC-X the massflows are $\phi_{m,I} = 4.619\,\mathrm{g/s}$ and $\phi_{m,X} = 4.891\,\mathrm{g/s}$.

3.3.2 Heat production by combustion in the secondary burner

The secondary burners are the main source of heat. The amount of heat produced can be found with equation 2.2.

For natural gas in the Netherlands, we find $\rho^0 = 0.833\,\mathrm{kg/m^3}$ and $\Delta h_c^0 = 31.65\,\mathrm{MJ/m^3}$.[6]

The actual amount of gas that is reacting in the second burner $\phi_{m,gas}$ is a known variable, found in table 3.3, and we find the heat production to be

$$P_e = \phi_{m,gas} \cdot \frac{\Delta h_c^0}{\rho^0} \tag{3.5}$$

Filling in the variables gives an energy production of $P_{e,I} = 7766\,\mathrm{J/s}$ and $P_{e,X} = 6851\,\mathrm{J/s}$ for respectively DJHC-I and DJHC-X.

3.3.3 Finding the average temperature of the coflow just after the secondary burner

Now both the coflow components and P_e are known, Δe_1 can be calculated. Since the control-volume is idealised, with height zero, the terms Δz and $\Delta\left(v^2\right)$ vanish from formula 2.5, leaving only

$$\Delta e_1 = \Delta h_1 = h_{in} - h_0 \tag{3.6}$$

The difference in enthalpy can be found by applying equation 2.9 to the coflow for the initial temperature T_0, and again for a (guessed) inlet temperature T_{in}. By iteration the temperature can be found such that the corresponding energy balance 3.1 is satisfied.

Of course, the initial temperature-profile of the coflow can never be totally smooth, but for convenience we will assume it to be, and have this temperature T_{in}.

Combining the found coflow compositions with the partial molar enthalpies $\overline{h_i}$ in equation 2.9, gives $h_{0,I} = 311.86\,\mathrm{J/g}$ and $h_{0,X} = 309.47\,\mathrm{J/g}$. (See Appendix B)

Note that for the partial enthalpy of Argon, the following formula, only applicable for monoatomic, ideal gases (because $\overline{c_p}$ is constant with temperature), has been used:

$$\overline{h_i} = \overline{c_p} \cdot T \tag{3.7}$$

where

$$\overline{c_p} = \frac{5}{2} \cdot R \tag{3.8}$$

with R the gas constant.

Combining formula 3.6 and 3.1 gives us the coflow enthalpy h_{in}:

$$h_{in} = \frac{P_e}{\phi_m} + h_0 \tag{3.9}$$

Since P_e and ϕ_m have been calculated earlier on for both coflow cases, we get $h_{in,I} = 1993.2\,\mathrm{J/g}$ and $h_{in,X} = 1710.2\,\mathrm{J/g}$.

By iteration (see Appendix B) we then find the inlet temperatures for both cases; $T_{in,I} = 1669\,\mathrm{K}$ and $T_{in,X} = 1474\,\mathrm{K}$.

3.4 Control Volume B

3.4.1 Loss of energy

As can be noticed in formula 3.2, the energy leaving the system per second $\dot{Q}$ equals the difference in concentration of energy over the controlvolume Δe_2 times the massflux. This difference can be split into kinetic energy, potential energy and enthalpy.

3.4.1.1 Kinetic energy

Because the massflux of the coflow is now a known variable, the average velocities v_{in} and v_{out}, needed for finding Δe (formula 2.5) can be found by equation 2.14 with the density $\rho(T)$ obviously being a temperature-dependent variable and the area perpendicular to the coflow A equal to

$$A = \pi \cdot \left[\left(\frac{D_1}{2} \right)^2 - \left(\frac{D_0}{2} \right)^2 \right] \tag{3.10}$$

Solving this with the data from table 3.1, gives $A = 4.97 \cdot 10^{-3}\,\mathrm{m}^2$.

The density can be found by applying the ideal gas model (unfortunately but inevitable, this method can give a small error, up to 5%)

$$p = \frac{\rho \cdot R \cdot T}{M} \tag{3.11}$$

Using the temperatures T_{in} and molar masses M found for the coflows and $p = 1.028\,\mathrm{bar}$ and $R = 8.3145\,\mathrm{J/mol{\cdot}K}$, gives $\rho_{in,I} = 209.1\,\mathrm{g/m^3}$ and $\rho_{in,X} = 237.8\,\mathrm{g/m^3}$.

Formula 2.14 then leads us to the initial average velocities of the coflow, using the massflows found before: $\langle v_{in,I} \rangle = 4.444\,\mathrm{m/s}$ and $\langle v_{in,X} \rangle = 4.138\,\mathrm{m/s}$

To find the average velocity $\langle v_{out} \rangle$ of the coflow at the higher end of the tube, we do not have to repeat this calculations; a LDA measurement of the velocity-profile will be available.

To be able to apply formula 2.16, we first need to rewrite this velocity-profile into a polynomic function $v(r)$. We can use *Microsoft Excel* to make fourth-order polynomial fits. Now we still lack information considering the density. But, since for all ideal gases the density is inversely proportional with the temperature as $\rho = \frac{C}{T}$, with C a constant, $\rho(r)$ can be replaced by a factor $\frac{1}{T}$.

A function for the temperature $T(r)$ can be recoved in the same way from CARS-measurements. Using integration limits $r_0 = \frac{D_0}{2}$ and $r_1 = \frac{D_1}{2}$ then yields

$$\langle v_{out} \rangle = \frac{\int_{r_0}^{r_1} \frac{r \cdot v}{T} \cdot dr}{\int_{r_0}^{r_1} \frac{r}{T} \cdot dr} \tag{3.12}$$

3.4.1.2 Potential energy

For the potential energy, Δz is simply equal to the tube length L.

3.4.1.3 Enthalpy

To calculate the change in enthalpyΔh, it is required to find the begin- and end-temperature(-profile) and the composition of the coflow. Since we know the composition and initial temperature of the coflow from section 3.3, the only variable that needs to be found is the temperature T_{out} at the exit of the annulus.

When the temperature-profile at the higher end of the tube is measured with CARS for both DJHC-I and DJHC-X, it will be able to find a related enthalpy-profile $h(r)$. Then, the average value $\langle h_{out} \rangle$ can be calculated by the method used in formula 2.18, once again replacing $\rho(r)$ with $\frac{1}{T}$, and integrating from r_0 to r_1.

This leads to

$$\langle h_{out} \rangle = \frac{\int_{r_0}^{r_1} \frac{r \cdot v \cdot h}{T} \cdot dr}{\int_{r_0}^{r_1} \frac{r \cdot v}{T} \cdot dr} \tag{3.13}$$

The relation between enthalpy h and temperature T for the mixtures is slightly nonlinear and can be found by the method described earlier on, using equation 2.9. This has been done for the range $990\,\mathrm{K} - 1680\,\mathrm{K}$ in Appendix B, resulting in graph 3.3.

3.4.2 Heat flux from the outer wall of the outer tube

At the outer wall, we can split the heat flux in a heat flux caused by radiation, and a heat flux by natural convection. The heat conduction in the iron wall of the tube in the vertical direction is neglected, because the thickness of the wall is very small, but more importantly, because the temperature gradient in the z-direction is far smaller than the temperature gradient in the radial direction.

The total heat leaving the outer wall per unit time $\dot{Q}_{wall}$ is

$$\dot{Q}_{wall} = \dot{Q}_{wall,r} + \dot{Q}_{wall,c} \tag{3.14}$$

3.4.2.1 Radiative heat flux at the outer wall

The heat flux caused by radiation $\dot{Q}_{wall,r}$ can be calculated by integrating 2.40 over the outer wall of the tube, since we estimate the pipe to be a grey body. Considering the walltemperature T_w to be dependent on the vertical coordinate z only and the total, hemispherical emissivity ϵ to be constant, gives rise to

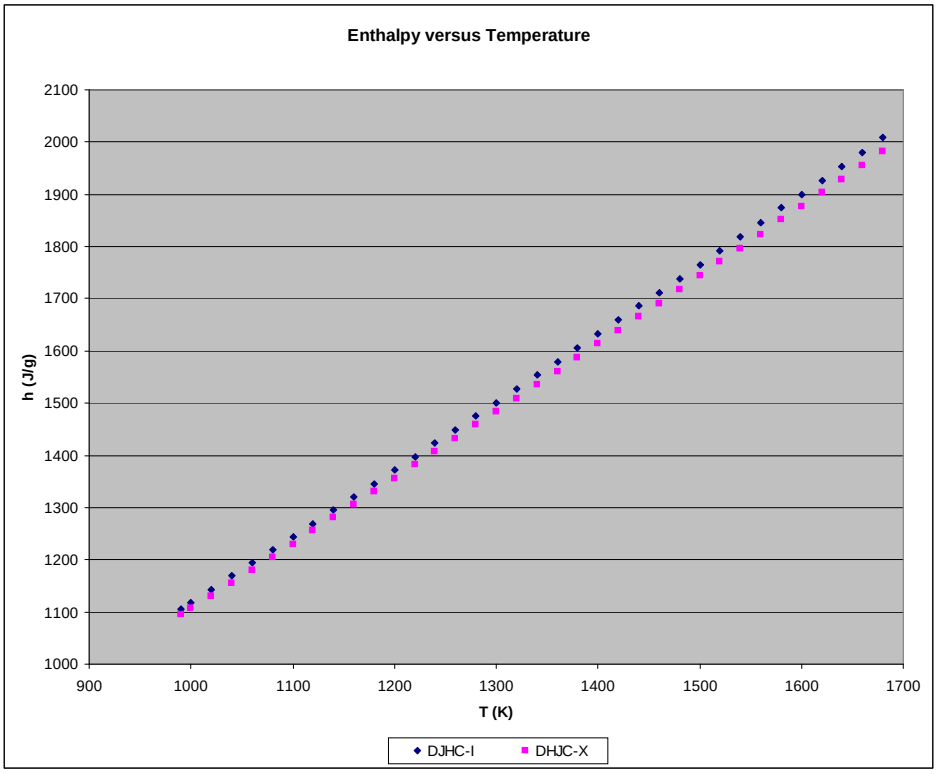

Figure 3.3: The found enthalpy h of the two different coflow mixtures, for different temperatures T.

$$\dot{Q}_{wall,r} = \int_0^{2\pi}\int_0^{L} \dot{q}_{wall,r} = \int_0^{2\pi}\int_0^{L} \epsilon\cdot\sigma\cdot T_w^4(z)\cdot dz\cdot d\varphi = \pi D_2\cdot\epsilon\cdot\sigma\cdot\int_0^{L} T_w^4(z)\cdot dz \quad (3.15)$$

Of course there is also inbound radiation from the room, but since its temperature T_{room} is estimated to be at least twice as low as the wall temperature, and the emissivity is smaller than 0.1, this shall be neglected.

3.4.2.2 Convective heat flux at the outer wall

The natural convection per unit area is found by combining equations 2.22 and 2.20 as

$$\dot{q}_{wall,c} = \langle Nu_w\rangle \cdot \frac{k}{L}\cdot \Delta T(z) \quad (3.16)$$

with $\Delta T(z) = T_w(z) - T_{room}$.

The total convective heat flux $\dot{Q}_{wall,c}$ can be found by integrating $\dot{q}_{wall,c}$ over the height and circumference of the tube:

$$\dot{Q}_{wall,c} = \int_0^{2\pi}\int_0^{L} \dot{q}_{wall,c} \cdot dz \cdot d\varphi = \pi D_2 \cdot \langle Nu_w \rangle \cdot \frac{k}{L} \cdot \int_0^{L} \left(T_w\left(z\right) - T_{room}\right) \cdot dz \quad (3.17)$$

where the average Nusselt number $\langle Nu_w \rangle$ is found by applying equation 2.45 or 2.47. To be able to apply these, we must assume an average walltemperature $\langle T_w \rangle$:

$$\langle T_w \rangle = \frac{\int_0^L T_w\left(z\right)}{L} \cdot dz \quad (3.18)$$

Also, the kinematic viscosity ν and thermal diffusivity α at that temperature need to be looked up.

3.4.3 Heat flux from the inner tube to the cooling air and the fuel duct

To complete the heat flux part of the energy balance, the heat leaving via the inner tube is required to be known. From [7] we find the heat flux $\dot{Q}_{cool}$ for an average temperature of 1300 K to be approximately $3 \cdot 10^2$ J/s. More accurate calculations could be made, but unfortunately the massflow $\phi_{m,cool}$ and temperature rise $\triangle T_{cool}$ of the coflow are not known. If they would be known, the heat flux could be found by

$$\dot{Q}_{cool} = \phi_{m,cool} \cdot \triangle T_{cool} \cdot c_p \quad (3.19)$$

with c_p being the heat capacity of air.

3.4.4 Heat fluxes in the annulus

To be able to get any quantification of the temperature profile in the annulus (the space where the hot coflow is flowing), it is necessary to get a better understanding of the heat fluxes pertaining to the hot coflow and its boundaries. A list of the significant heat fluxes:

- Conduction within the outer tube
- Driven convection between the hot coflow and the outer tube
- Driven convection between the hot coflow and the inner tube
- Radiative heat transfer between the inner tube and outer tube, where the hot coflow is a participating medium
- Conductive heat transfer within the coflow

Because the temperature of the inside of the outer tube (at D_1) is easily found, this shall be the starting point.

3.4.4.1 Finding the temperature at the inside of the outer tube

Within the outer tube heat is flowing. Because a steady-state system is considered and vertical conduction in the tube is neglected, the sum of heat fluxes leaving the outer tube from the outer wall is equal to the amount of heat $\dot{q}_{wall,conduct}$ surpassing the wall :

$$\dot{q}_{wall,conduct} = \dot{q}_{wall,c} + \dot{q}_{wall,r} \tag{3.20}$$

Then, using equation 2.29, the temperature at the inside of the outer tube can be found.

3.4.4.2 Driven convection inside the annulus

Using section 2.2.4, formulae for the heat flux due to convection are easily found. Since we assume the flow to be laminar (with $v = 4.0\,\mathrm{m/s}$, $D = D_1 = 82.5\,\mathrm{mm}$ and $\nu_{air}\,(1250\,\mathrm{K}) = 1731 \cdot 10^{-6}\,\mathrm{m^2/s}$, we find $Re = 1906$), we find the convective heat fluxes

$$\dot{q}_{convection} = Nu \cdot \frac{k}{D_1} \cdot \triangle T \tag{3.21}$$

with the Nusselt number for the inward heat flux (to the cooling duct) $\langle Nu \rangle_0 = 7.86$ and for the outward flux $\langle Nu \rangle_1 = 3.66$.

3.4.4.3 Conduction within the annulus

To calculate the conduction within the coflow, we consider the velocity to be equal in the annulus. Calculation is only possible with some numerical method, using the formula of radial conduction found before 2.29. Dividing the cylinder in rings, gives the conduction from inner radius r_i to outer radius r_j as

$$\dot{q}_{conduction} = -\frac{k}{r_j \cdot \ln\left(r_i/r_j\right)} \cdot (T_i - T_j)$$

3.4.4.4 Radiation within the annulus

For the radiation originating from the outer wall, view factors are needed.

Using the formulae in section 2.2.2.1 gives $F_{2-1} = 0.27$ and $F_{2-2} = 0.73$.

The directional heat flux originating from a point at the surface is then found by integrating 2.44 over all wavelengths.

$$\dot{q}\left(\hat{s}\right) = \int_0^\infty I_\eta\left(\tau_\eta\right) \cdot d\eta = \int_0^\infty \left[I_\eta\left(0\right) \cdot e^{-\tau_\eta} + \int_0^{\tau_\eta} I_{b\eta}\left(\tau'_\eta\right) \cdot e^{-\left(\tau_\eta - \tau'_\eta\right)} \cdot d\tau'_\eta \right] \cdot d\eta \tag{3.22}$$

When summing up all directional heat fluxes that are directed to a single surface area, the amount of energy arriving at that area is found (which must, together with the added energy by driven convection, be equal to the heat flux

leaving that area by radiation and the heat flux to the room. If this is done for all surface areas, insight of the temperature field of the coflow can be gained.

3.5 Measurement of the temperature of the outer tube

As explained earlier on, the temperature at the tube wall has to be measured to be able to calculate all the heat fluxes and temperature profiles.

A simple configuration of five thermocouples in combination with a digital multimeter (single input) was chosen.

Normally the thermocouples would be soldered to the tube, but because temperatures of several hundreds degrees Celcius were expected, spot welding was used.

3.5.1 Spot Welding

Spot welding is a process in which two metals are forged together by the conversion of a large current (several thousand ampères) into heat. Because the contact resistance between the two metals is usually higher than the internal resistance, the contact point of the two metals heats up and melts eventually, after several milliseconds, forming a weld. Typically, spot welding is used for metals of only several millimeters thickness.

Next, the question remained if the tube's surface needed to be treated in some way. Several sized holes were drilled in the metal, but welding inside a hole proved to be a too cumbersome job. In the end, the thermocouples were just welded in little depressions on the surface.

3.5.2 Choice of thermocouple type

When picking a thermocouple type, one wants its sensitivity to be as high as possible for getting high resolution measurements. Because the exact range of temperature was still unknown, the K-type (chromel-alumel), stable at temperatures up to 1300 °C , was chosen from table 2.2. The corresponding thermocouple reference table is found in Appendix C.

3.5.3 Thermocouple calibration

Before taking the thermocouple into use, it must be calibrated. In order to do this, the hot joint was held in boiling water, while the cold joint was cooled by melting ice, such that $T_2 = 0\,°\mathrm{C}$. With the pressure being 1.028 bar at that time, the temperature of the hot joint was found to be $T_1 = 100.3\,°\mathrm{C}$. [9] The measured thermocouple voltage was 4.099 mV, resulting in a sensitivity of $40.9\,\mu\mathrm{V/K}$.

A lot more accurate than using the sensitivity for further calculations, is the use of the reference table in Appendix C. For T_1 a voltage of 4.1086 mV can be found. Hence, for all future measurements, the voltages in the reference table will be scaled with $\frac{4.099}{4.1086} = 0.9977$.

Chapter 4

Results

4.1 Energy Balance A

The first energy balance (equation 3.1), covering the adiabatic combustion of natural gas in the secondary burner at the bottom of the DJHC, was already solved by doing calculations with the provided volume fluxes of the two cases, DJHC-I and DJHC-X. The resulting temperature, enthalpy and massfluxes are given in table 4.1.

	DJHC-I	DJHC-X
$\phi_{m,air}$	4.415 g/s	4.711 g/s
$\phi_{m,gas}$	0.2044 g/s	0.1803 g/s
h_{in}	1993.2 J/g	1710.2 J/g
T_{in}	1669 K	1474 K

Table 4.1: Coflow enthalpy h_{in} and temperature T_{in} directly after the secondary combustion, including the massfluxes of air $\phi_{m,air}$ and natural gas $\phi_{m,gas}$, for both case DJHC-I and DJHC-X.

4.2 Energy Balance B

4.2.1 Temperature- and velocity-profiles

As noted before, data from LDA and CARS are needed to solve the energy balance that covers the annulus containing the coflow (equation 3.2).

Both the temperature and velocity measurements [12] can be found in Appendix D, with the associated graphs (4.1, 4.2) showing non-uniform profiles.

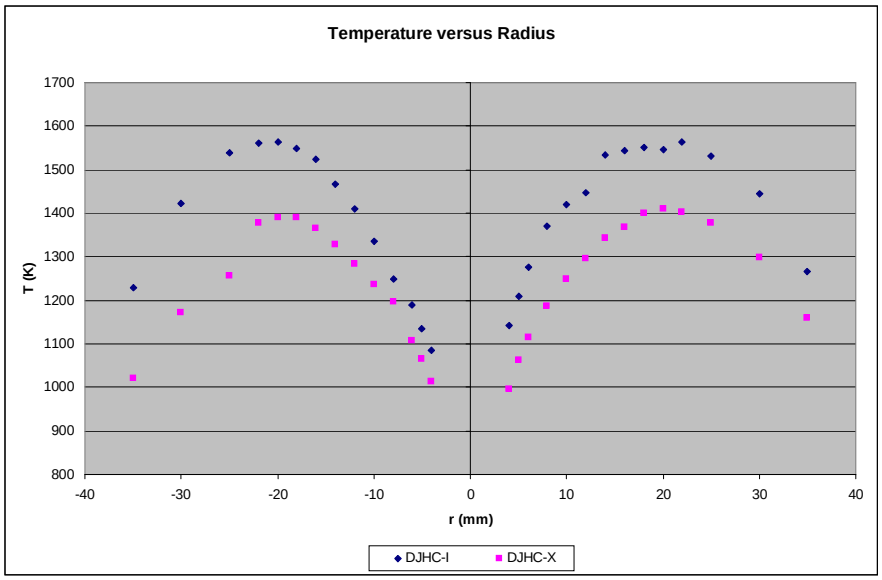

Figure 4.1: Temperature T measurements for the coflow at $3\,\mathrm{mm}$ above the pipe for different radii r, for both cases.

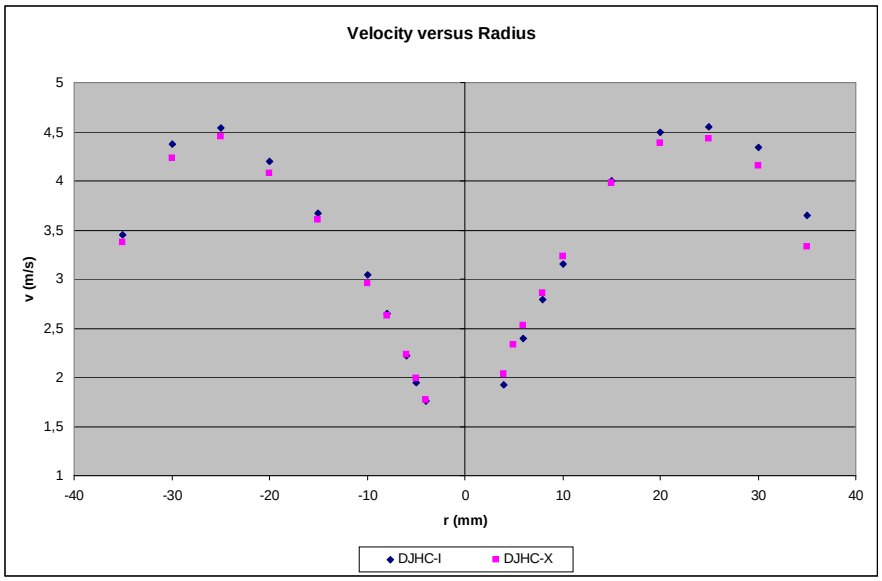

Figure 4.2: Velocity v measurements for the coflow at $3\,\mathrm{mm}$ above the pipe for different radii r, for both cases.

4.2.2 Enthalpy-profile

Using the calculated enthalpy-temperature tables from Appendix B for both mixtures of the coflow, the enthalpies can be found for the measured temperatures at the top, resulting in an enthalpy-profile as shown in figure 4.3. The full dataset can be found in Appendix D.

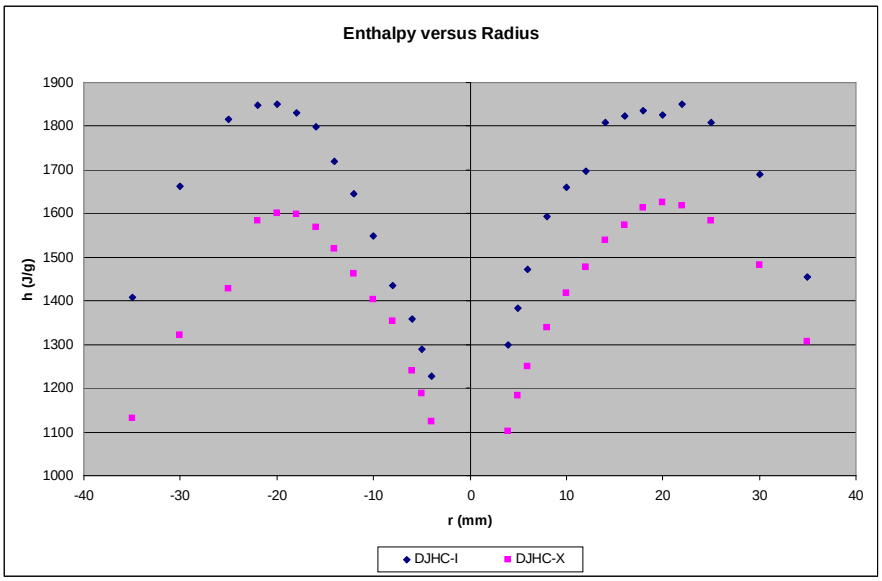

Figure 4.3: Enthalpy h calculations for the coflow at $3\,\mathrm{mm}$ above the pipe for different radii r, for both cases.

4.2.3 Coflow characteristics

When applying the averaging method from formulae 3.12 and 3.13, the average values for v_{out} and h_{out} are found.

We converted the enthalpy-, temperature- and velocity-profiles into fourth-order polynomials using *Maple 12*. The polynomials are plotted together with the datapoints in the graphs in Appendix E.

	DJHC-I	DJHC-X
ϕ_m	$4.619\,\mathrm{g/s}$	$4.891\,\mathrm{g/s}$
$\langle v_{in} \rangle$	$4.444\,\mathrm{m/s}$	$4.138\,\mathrm{m/s}$
$\langle v_{out} \rangle$	$3.97\,\mathrm{m/s}$	$3.84\,\mathrm{m/s}$
$\langle h_{out} \rangle$	$1.67\,\mathrm{kJ/g}$	$1.43\,\mathrm{kJ/g}$
h_{in}	$1.9932\,\mathrm{kJ/g}$	$1.7102\,\mathrm{kJ/g}$

Table 4.2: The found massflux ϕ_m, average velocities $\langle v_{in} \rangle$ and $\langle v_{out} \rangle$, and average high-end enthalpy $\langle h_{out} \rangle$ of the coflow.

4.2.4 Solving the balance

Finally, using the information from the previous sections, balance 3.2 can be filled in. The balance gives us the total heat loss of the coflow between secondary

combustion and the departing of the pipe per second, $\dot{Q}$.

We find $\dot{Q}_I = 1429.6\,\mathrm{J/s}$ and $\dot{Q}_X = 1299.5\,\mathrm{J/s}$.

In the following section we will calculate the heat losses one by one, and check if they equal $\dot{Q}$ when summed.

4.3 Heat flux at the outer wall

For both case I and case X, 2 temperature-measurements have been done at the DJHC's wall with thermocouples. Using the correction factor calculated in subsection 3.5.3 and the thermocouple tables in Appendix C enables us to rewrite the voltages into temperatures. The datasets can be seen in Appendix F and are plotted in figure 4.4.

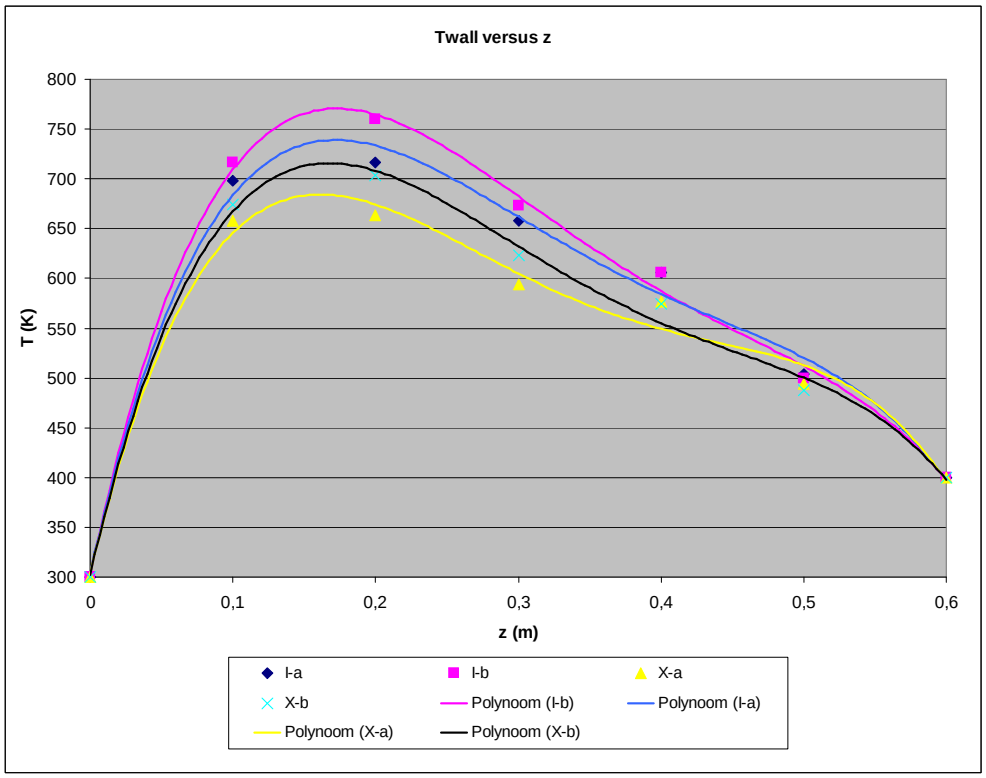

Figure 4.4: Measured wall temperatures T_w for coflow I and X. All measurements (a and b) are plotted, together with their polynomial fits.

To approximate the wall-temperature T_w as function of the height z, *Microsoft Excel* was used to make a polynomial fit. Unfortunately, using the thermocouple measurements up $z = 0.5\,\mathrm{m}$ leads to a fit not in any agreement with the CARS measurements at the top ($z = 0.6\,\mathrm{m}$), Therefore the fit was based on the thermocouple measurements combined with the CARS measurements from Appendix D at $z = 0.56\,\mathrm{m}$. Then, using 3.18, average temperatures were found for each of the four datasets.

With this average temperature $\langle T_w \rangle$, a corresponding thermal diffusivity and kinematic viscosity for air were found by cubic interpolation of the data from

[4], listable in table 4.3.

Furthermore, the room temperature was measured to be 297 K.

Case	$\langle T_w \rangle$	α	ν
I-a	600 K	$73.11 \cdot 10^{-6}\,\mathrm{m^2/s}$	$50.50 \cdot 10^{-6}\,\mathrm{m^2/s}$
I-b	613 K	$75.65 \cdot 10^{-6}\,\mathrm{m^2/s}$	$52.32 \cdot 10^{-6}\,\mathrm{m^2/s}$
X-a	567 K	$66.74 \cdot 10^{-6}\,\mathrm{m^2/s}$	$45.98 \cdot 10^{-6}\,\mathrm{m^2/s}$
X-b	580 K	$69.23 \cdot 10^{-6}\,\mathrm{m^2/s}$	$47.74 \cdot 10^{-6}\,\mathrm{m^2/s}$

Table 4.3: Averaged temperature and corresponding thermal diffusivity α and kinematic viscosity ν, for mixtures I and X.

Using formula 3.15 with total, hemispherical emissivity $\epsilon = 0.6$[4] enables us to compute the value of the heat flux at the wall caused by radiation, $\dot{Q}_r$.

Also, applying formula 3.17 with air's thermal conductivity $k\,(T)$[4] gives us the convective heat flux $\dot{Q}_c$. In table 4.4 these heat fluxes are listed, together with the total heat flux from the DJHC wall $\dot{Q}_{wall}$ and the total heat loss $\dot{Q}$.

In figure 4.5 the heat flux leaving the wall per unit area is plotted as function of height.

Case	$\dot{Q}_r$	$\dot{Q}_c$	$\dot{Q}_{wall}$	$\dot{Q}_{cool}$	$\dot{Q}$
I-a	870 J/s	308 J/s	1179 J/s	0.3 kJ/s	1.5 kJ/s
I-b	975 J/s	324 J/s	1298 J/s	0.3 kJ/s	1.6 kJ/s
X-a	666 J/s	270 J/s	936 J/s	0.3 kJ/s	1.2 kJ/s
X-b	753 J/s	286 J/s	1039 J/s	0.3 kJ/s	1.3 kJ/s

Table 4.4: List of the calculated radiative and convective heat fluxes $\dot{Q}_r$ and $\dot{Q}_c$, the total heat flux from the outer wall and to the inner duct $\dot{Q}_{wall}$ and $\dot{Q}_{cool}$, and the total heat flux leaving the annulus $\dot{Q}$.

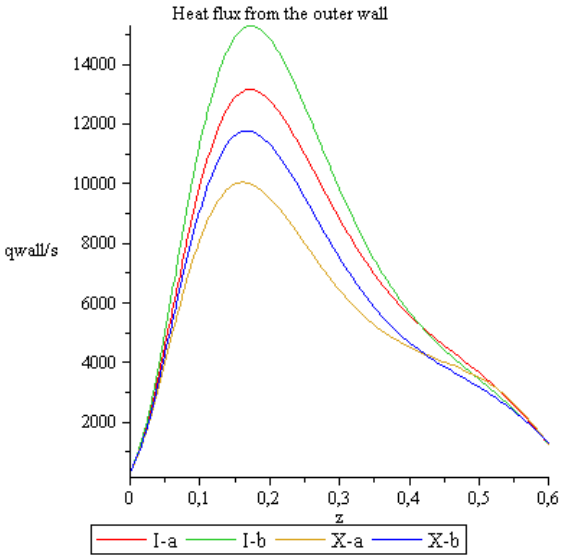

Figure 4.5: Heat flux from the wall per unit area $\dot{q}_{wall}$ for all cases.

4.4 Temperature inside the annulus

Using relation 3.20 and the parameters found in section 4.3 gives the temperature difference $\triangle T_{wall}$ between the inside and outside of the outer wall. As can be seen in figure 4.6, this difference is generally less than 1 K, so the temperature-profile of the inside of the outer burner wall is nearly the same as the measured T_{wall} at the outside.

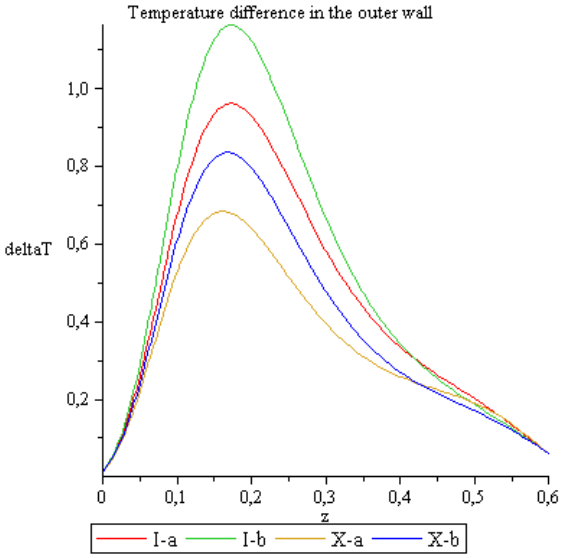

Figure 4.6: Temperature difference inside the outer wall $\triangle T_{wall}$ versus height z for the four found temperatureprofiles.

Because only the total heat flux to the cooling gas is known, it is hard to produce the temperature profile along the inner wall of the burner. An option is to assume the profile to be decreasing linearly from it's maximum value T_{in} (table 4.1) at $z = 0\,\mathrm{m}$ to the minimum of T_{CARS} (1 mm) from Appendix D at $z = 0.6\,\mathrm{m}$.

This results in the temperatureprofiles $T(r, z)$ at the boundaries and constants in 4.1:

Algorithm 4.1 Simplified input for a numerical solver, numbers from measurement b are used.

Properties

$$D_1 = 2r_1 = 0.0825\,\mathrm{m}$$

$$D_0 = 2r_0 = 0.022\,\mathrm{m}$$

$$L = 0.6\,\mathrm{m}$$

$$\langle Nu \rangle_0 = 7.86$$

$$\langle Nu \rangle_1 = 3.66$$

thermodynamic properties of the coflow

Boundary conditions for Coflow I

$$T_I\left(r = r_1, z\right) = -38182z^4 + 58874z^3 - 32630z^2 + 6789.9z + 301.84$$

$$T_I\left(r = r_0, z\right) = 1669 - 1932z$$

$$T_I\left(r, z = 0\right) = 1669$$

$$T_I\left(r, z = L\right) = -0.0017161r^4 + 0.14346r^3 - 5.5218r^2 + 104.01r + 812.38$$

Boundary conditions for Coflow X

$$T_X\left(r = r_1, z\right) = -38598z^4 + 57846z^3 - 30884z^2 + 6202.2z + 301.91$$

$$T_X\left(r = r_0, z\right) = 1474 - 1643z$$

$$T_X\left(r, z = 0\right) = 1474$$

$$T_X\left(r, z = L\right) = -0.00030619r^4 + 0.031540r^3 - 2.3973r^2 + 69.639r + 765.34$$

Heat Fluxes

$$\dot{q}_{conduction} = -\frac{k}{r_j \cdot \ln\left(r_i/r_j\right)} \cdot \left(T_i - T_j\right)$$

$$\dot{q}_{convection} = Nu \cdot \frac{k}{D_1} \cdot \triangle T$$

$$\dot{q}_{radiation}\left(\hat{s}\right) = \int_0^\infty I_\eta\left(\tau_\eta\right) \cdot d\eta = \int_0^\infty \left[I_\eta\left(0\right) \cdot e^{-\tau_\eta} + \int_0^{\tau_\eta} I_{b\eta}\left(\tau'_\eta\right) \cdot e^{-\left(\tau_\eta - \tau'_\eta\right)} \cdot d\tau'_\eta \right] \cdot d\eta$$

Chapter 5

Conclusions

The total heat fluxes that have been calculated using thermocouples were 1.6 kJ/s and 1.3 kJ/s for respectively mixture DJHC-I and DJHC-X and are very similar to the total heat fluxes that were found using the LDA and CARS measurements (1.43 kJ/s and 1.30 kJ/s).

Comparing this energy loss to the heat production when the combustion is considered adiabatically (giving productions of respectively 7.77 kJ/s and 6.58 kJ/s), results in a heat loss of respectively 19 % and 21 % for mixture DJHC-I, and 18 % and 19 % for mixture DJHC-X.

As expected, most of the heat loss was due to radiation (around 60 % of the total, for both mixtures), although the amount of heat loss by cooling and free convection is not negligible, both contributing around 20 % of the total heat loss.

The total heat to the cooling air was calculated to be 0.3 kJ/s for both air-gas mixtures, while the total heat to the surroundings was found to be as high as 1.3 kJ/s and 1.0 kJ/s, for respectively mixture I and X.

Chapter 6

Discussion

In this experiment, a lot of data was not too accurately measured, resulting in a not as accurate heat fluxes and temperatures as expected.

For example, if the thermocouples would be placed just a millimeter from the DJHC wall, this mattered dozens of degrees Kelvin. Also, around the bottom and top of the pipe, the temperature profile on the wall was not known too well (error up to 50 K)

Another important inaccuracy is the total, hemispherical emissivity. Literature listed this to be in the range $0.5 - 0.8$, and since the radiative heat flux is more than half of the total heat flux, this matters a lot. Furthermore, the iron has been considered a grey emitter.

Lastly, the heat flux due to cooling is a very crude estimate, and an error of 50 % would not be unlikely.

Next, the calculations to internal energy have been made while doing a lot of estimates.

First of all, the natural gas was assumed to combust adiabatically, without production of NO_x, and the resulting temperature to be constant for that height.

Also, the pressure was considered constant everywhere, and the density of the coflow to behave like an ideal gas' density, that is, linear with T^{-1}.

Then, at the top end of the DJHC, CARS-measurements were used. Unfortunately, these were not availabe at a lower height than at 3 mm above the fuel duct (so 18 mm above the top), which will have led to a slightly lower temperature profile.

Lastly, the effect of the distribution plate inside the annulus was neglected.

Some recommendations for interesting measurements and calculations that will give more insight to some heat fluxes are:

- Measuring the temperature gain and massflux of the cooling air, in that way being able to calculate the heat flux from the coflow to the cooling duct very accurately.
- Measuring the total hemispherical emissivity of the burner pipe with some device.
- Securing some of the coflow gases and studying it's components and material properties such as density, enthalpy and total emissivity.
- Using a numerical solver to calculated the temperature profile of the coflow in 3-dimensions, using the inlet, outlet and outer wall temperatures, the velocity profile and the formulae for driven convection to the walls, conduction inside the coflow, and radiation between the annulus' walls, where the coflow is a participating medium.

Bibliography

[1] H. van der Akker, R. Mudde, *Fysische Transportverschijnselen I*, VSSD 2005

[2] M. Modest, *Radiative Heat Transfer*, Academic Press, 1993

[3] L. Janssen, M. Warmoeskerken, *Transport Phenomena Data Companion*, VSSD, 2006

[4] M. Kaviani, *Principles of Heat Transfer*, John Wiley & Sons. Inc., 2002

[5] E. Angad Gaur, E. Lagendijk, *Fysische Transportverschijnselen*, TU Delft, 2005

[6] Wikipedia, the free encyclopedia, *Heat*, from http://en.wikipedia.com/heat

[7] E. Oldenhof, *Operational Conditions of Delft/Adelaide JHC Burner*, TU Delft, 2006

[8] E. Oldenhof, *The Development and Rationale of the Delft Jet-in-Hot-Coflow Burner*, TU Delft, 2007

[9] M. Moran, H. Shapiro, *Fundamentals of Engineering Thermodynamics*, John Wiley & Sons Ltd, 1998

[10] E. Oldenhof, M. Tummers, E. Van Veen, D. Roekaerts, *Ignition Kernel Statistics of Delft Jet-in-Hot-Coflow Flames*, Department of Multi-Scale Physics, Proceedings European Combustion Meeting, 2009

[11] D. Williams, *Earth Fact Sheet*, http://nssdc.gsfc.nasa.gov/planetary/factsheet/earthfact.html, NASA, 2007

[12] LDA & CARS measurements, by E. Oldenhof, TU Delft, 2008-2009

[13] *N.I.S.T. Type K Reference Tables*, from http://www.omega.com/temperature/Z/pdf/z204-206.pdf

Appendix A

Coflow

This appendix lists the available data on the composition of the different streams; natural gas, air and coflow.

gas	i	Yi	Mi	Mi*Yi	ni	mi	mfi
	N2	14,32%	28,01	4,0115	0,0016	0,0440	21,53%
	CO2	0,89%	44,01	0,3917	0,0001	0,0043	2,10%
	O2	0,01%	32,00	0,0032	0,0000	0,0000	0,02%
	CH4	81,29%	16,04	13,0389	0,0089	0,1430	69,97%
	C2H6	2,87%	30,07	0,8630	0,0003	0,0095	4,63%
	C3H8	0,38%	44,10	0,1676	0,0000	0,0018	0,90%
	C4H10	0,15%	58,12	0,0872	0,0000	0,0010	0,47%
	C5H12	0,04%	72,15	0,0289	0,0000	0,0003	0,15%
	C6H14	0,05%	86,18	0,0431	0,0000	0,0005	0,23%
		100,00%		18,6350 M	0,0110 n	0,2044 m	100,00%

i	ni
C	0,0099
H	0,0382
O	0,0002
N	0,0031

Air	i	Yi	Mi	Mi*Yi	ni	mi	mfi
	N2	78,08%	28,01	21,8740	0,1190	3,3340	75,51%
	O2	20,95%	32,00	6,7025	0,0319	1,0216	23,14%
	Ar	0,93%	39,98	0,3735	0,0014	0,0569	1,29%
	CO2	0,04%	44,01	0,0167	0,0001	0,0025	0,06%
		100,00%		28,9666 M	0,1524 n	4,4150 m	100,00%

i	ni
C	0,0001
O	0,0640
N	0,2380
Ar	0,0014

coflow I	i	Yi	Mi	Mi*Yi	ni
	Ar	0,87%	39,98	0,3478	0,0014
	CO2	6,08%	44,01	2,6757	0,0099
	H2O	11,67%	18,02	2,1027	0,0191
	N2	73,69%	28,01	20,6431	0,1206
	O2	7,69%	32,00	2,4612	0,0126
		100,00%		28,2306 M	0,1636 n

i	ni
C	0,0099
H	0,0382
O	0,0642
N	0,2412
Ar	0,0014

	gas	air			23,5 Celcius	0,0 Celcius
l/min	16,1	224		rho gas	0,7619	0,833
l/s	0,2683333	3,733333		rho air	1,1826	1,293
g/s	0,2044364	4,415033	4,6195			

R	8,3145
monoatomic Cp	20,78625

Table A.1: Coflow Properties for DJHC-I [10, 3, 9, 6, 11]

gas	i	Yi	Mi	Mi*Yi	ni	mi	mfi
	N2	14,32%	28,01	4,0115	0,0014	0,0388	21,53%
	CO2	0,89%	44,01	0,3917	0,0001	0,0038	2,10%
	O2	0,01%	32,00	0,0032	0,0000	0,0000	0,02%
	CH4	81,29%	16,04	13,0389	0,0079	0,1262	69,97%
	C2H6	2,87%	30,07	0,8630	0,0003	0,0084	4,63%
	C3H8	0,38%	44,10	0,1676	0,0000	0,0016	0,90%
	C4H10	0,15%	58,12	0,0872	0,0000	0,0008	0,47%
	C5H12	0,04%	72,15	0,0289	0,0000	0,0003	0,15%
	C6H14	0,05%	86,18	0,0431	0,0000	0,0004	0,23%
		100,00%		18,6350	0,0097	0,1803	100,00%
				M	n	m	

i	ni
C	0,0087
H	0,0337
O	0,0002
N	0,0028

Air	i	Yi	Mi	Mi*Yi	ni	mi	mfi
	N2	78,08%	28,01	21,8740	0,1270	3,5572	75,51%
	O2	20,95%	32,00	6,7025	0,0341	1,0900	23,14%
	Ar	0,93%	39,98	0,3735	0,0015	0,0607	1,29%
	CO2	0,04%	44,01	0,0167	0,0001	0,0027	0,06%
		100,00%		28,9666	0,1626	4,7107	100,00%
				M	n	m	

i	ni
C	0,0001
O	0,0683
N	0,2540
Ar	0,0015

coflow X	i	Yi	Mi	Mi*Yi	ni
	Ar	0,88%	39,98	0,3520	0,0015
	CO2	5,09%	44,01	2,2412	0,0088
	H2O	9,76%	18,02	1,7590	0,0168
	N2	74,41%	28,01	20,8442	0,1284
	O2	9,86%	32,00	3,1543	0,0170
		100,00%		28,3508	0,1725
				M	n

i	ni
C	0,0088
H	0,0337
O	0,0684
N	0,2567
Ar	0,0015

	gas	air			23,5 Celcius	0,0 Celcius
l/min	14,2	239		rho gas	0,7619	0,833
l/s	0,2366667	3,983333		rho air	1,1826	1,293
g/s	0,1803104	4,710683	4,8910			

R	8,3145
monoatomic Cp	20,78625

Table A.2: Coflow Properties for DJHC-X [10, 3, 9, 6, 11]

Appendix B

Enthalpy-Temperature relations

	T (K)	297	990	1000	1020	1040	1060	1080	1100	1120
0,87%	**Ar**	6174	20578	20786	21202	21618	22033	22449	22865	23281
6,08%	**CO2**	9326	42226	42769	43859	44953	46051	47153	48258	49369
11,67%	**H2O**	9870	35472	35882	36709	37542	38380	39223	40071	40923
73,69%	**N2**	8639	29803	30129	30784	31442	32101	32762	33426	34092
7,69%	**O2**	8652	31041	31389	32088	32789	33490	34194	34899	35606
M = 28,2306	**h (J/g)**	311,86	1106,42	1118,80	1143,70	1168,71	1193,78	1218,94	1244,20	1269,56

T (K)	1140	1160	1180	1200	1220	1240	1260	1280	1300	1320
Ar	23696	24112	24528	24944	25359	25775	26191	26606	27022	27438
CO2	50484	51602	52724	53848	54977	56108	57244	58381	59522	60666
H2O	41780	42642	43509	44380	45256	46137	47022	47912	48807	49707
N2	34760	35430	36104	36777	37452	38129	38807	39488	40170	40853
O2	36314	37023	37734	38447	39162	39877	40594	41312	42033	42753
h (J/g)	1294,99	1320,51	1346,17	1371,83	1397,58	1423,40	1449,29	1475,28	1501,33	1527,43

T (K)	1340	1360	1380	1400	1420	1440	1460	1480	1500	1520
Ar	27854	28269	28685	29101	29516	29932	30348	30764	31179	31595
CO2	61813	62963	64116	65271	66427	67586	68748	69911	71078	72246
H2O	50612	51521	52434	53351	54273	55198	56128	57062	57999	58942
N2	41539	42227	42915	43605	44295	44988	45682	46377	47073	47771
O2	43475	44198	44923	45648	46374	47102	47831	48561	49292	50024
h (J/g)	1553,64	1579,93	1606,25	1632,64	1659,06	1685,58	1712,16	1738,78	1765,46	1792,21

T (K)	1540	1560	1580	1600	1620	1640	1660	1680
Ar	32011	32427	32842	33258	33674	34089	34505	34921
CO2	73417	74590	76767	76944	78123	79303	80486	81670
H2O	59888	60838	61792	62748	63709	64675	65643	66614
N2	48470	49168	49869	50571	51275	51980	52686	53393
O2	50756	51490	52224	52961	53696	54434	55172	55912
h (J/g)	1819,01	1845,81	1874,87	1899,66	1926,68	1953,76	1980,87	2008,04

Table B.1: Relation between temperature $T\,(\mathrm{K})$ and enthalpy $h\,(^{\mathrm{J}}/_{\mathrm{g}})$ for coflow mixture I, using the partial molar enthalpies $\overline{h_i}$ of the components. [9]

	T (K)	297	990	1000	1020	1040	1060	1080	1100	1120
0,88%	**Ar**	6174	20578	20786	21202	21618	22033	22449	22865	23281
5,09%	**CO2**	9326	42226	42769	43859	44953	46051	47153	48258	49369
9,76%	**H2O**	9870	35472	35882	36709	37542	38380	39223	40071	40923
74,41%	**N2**	8639	29803	30129	30784	31442	32101	32762	33426	34092
9,86%	**O2**	8652	31041	31389	32088	32789	33490	34194	34899	35606
M = 28,3508	**h (J/g)**	309,47	1094,50	1106,72	1131,27	1155,94	1180,66	1205,47	1230,38	1255,38

T (K)	1140	1160	1180	1200	1220	1240	1260	1280	1300	1320
Ar	23696	24112	24528	24944	25359	25775	26191	26606	27022	27438
CO2	50484	51602	52724	53848	54977	56108	57244	58381	59522	60666
H2O	41780	42642	43509	44380	45256	46137	47022	47912	48807	49707
N2	34760	35430	36104	36777	37452	38129	38807	39488	40170	40853
O2	36314	37023	37734	38447	39162	39877	40594	41312	42033	42753
h (J/g)	1280,45	1305,61	1330,90	1356,19	1381,56	1407,01	1432,52	1458,12	1483,79	1509,50

T (K)	1340	1360	1380	1400	1420	1440	1460	1480	1500	1520
Ar	27854	28269	28685	29101	29516	29932	30348	30764	31179	31595
CO2	61813	62963	64116	65271	66427	67586	68748	69911	71078	72246
H2O	50612	51521	52434	53351	54273	55198	56128	57062	57999	58942
N2	41539	42227	42915	43605	44295	44988	45682	46377	47073	47771
O2	43475	44198	44923	45648	46374	47102	47831	48561	49292	50024
h (J/g)	1535,32	1561,22	1587,14	1613,13	1639,14	1665,26	1691,42	1717,64	1743,90	1770,24

T (K)	1540	1560	1580	1600	1620	1640	1660	1680
Ar	32011	32427	32842	33258	33674	34089	34505	34921
CO2	73417	74590	76767	76944	78123	79303	80486	81670
H2O	59888	60838	61792	62748	63709	64675	65643	66614
N2	48470	49168	49869	50571	51275	51980	52686	53393
O2	50756	51490	52224	52961	53696	54434	55172	55912
h (J/g)	1796,62	1823,00	1851,27	1876,00	1902,58	1929,23	1955,91	1982,64

Table B.2: Relation between temperature $T\,(\mathrm{K})$ and enthalpy $h\,(^{\mathrm{J}}/_{\mathrm{g}})$ for coflow mixture X, using the partial molar enthalpies $\overline{h_i}$ of the components. [9]

Appendix C

Type-K Thermocouple

Revised Thermocouple Reference Tables

TYPE K

Reference Tables
N.I.S.T. Monograph 175
Revised to ITS-90

Thermocouple Grade

Nickel-Chromium
vs.
Nickel-Aluminum

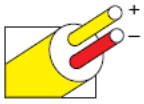

Extension Grade

MAXIMUM TEMPERATURE RANGE
Thermocouple Grade
– 328 to 2282°F
– 200 to 1250°C
Extension Grade
32 to 392°F
0 to 200°C
LIMITS OF ERROR
(whichever is greater)
Standard: 2.2°C or 0.75% Above 0°C
2.2°C or 2.0% Below 0°C
Special: 1.1°C or 0.4%
COMMENTS, BARE WIRE ENVIRONMENT:
Clean Oxidizing and Inert; Limited Use in Vacuum or Reducing; Wide Temperature Range; Most Popular Calibration
TEMPERATURE IN DEGREES °C
REFERENCE JUNCTION AT 0°C

Thermoelectric Voltage in Millivolts

°C	0	1	2	3	4	5	6	7	8	9	10	°C
800	33.275	33.316	33.357	33.398	33.439	33.480	33.521	33.562	33.603	33.644	33.685	800
810	33.685	33.726	33.767	33.808	33.848	33.889	33.930	33.971	34.012	34.053	34.093	810
820	34.093	34.134	34.175	34.216	34.257	34.297	34.338	34.379	34.420	34.460	34.501	820
830	34.501	34.542	34.582	34.623	34.664	34.704	34.745	34.786	34.826	34.867	34.908	830
840	34.908	34.948	34.989	35.029	35.070	35.110	35.151	35.192	35.232	35.273	35.313	840
850	35.313	35.354	35.394	35.435	35.475	35.516	35.556	35.596	35.637	35.677	35.718	850
860	35.718	35.758	35.798	35.839	35.879	35.920	35.960	36.000	36.041	36.081	36.121	860
870	36.121	36.162	36.202	36.242	36.282	36.323	36.363	36.403	36.443	36.484	36.524	870
880	36.524	36.564	36.604	36.644	36.685	36.725	36.765	36.805	36.845	36.885	36.925	880
890	36.925	36.965	37.006	37.046	37.086	37.126	37.166	37.206	37.246	37.286	37.326	890
900	37.326	37.366	37.406	37.446	37.486	37.526	37.566	37.606	37.646	37.686	37.725	900
910	37.725	37.765	37.805	37.845	37.885	37.925	37.965	38.005	38.044	38.084	38.124	910
920	38.124	38.164	38.204	38.243	38.283	38.323	38.363	38.402	38.442	38.482	38.522	920
930	38.522	38.561	38.601	38.641	38.680	38.720	38.760	38.799	38.839	38.878	38.918	930
940	38.918	38.958	38.997	39.037	39.076	39.116	39.155	39.195	39.235	39.274	39.314	940
950	39.314	39.353	39.393	39.432	39.471	39.511	39.550	39.590	39.629	39.669	39.708	950
960	39.708	39.747	39.787	39.826	39.866	39.905	39.944	39.984	40.023	40.062	40.101	960
970	40.101	40.141	40.180	40.219	40.259	40.298	40.337	40.376	40.415	40.455	40.494	970
980	40.494	40.533	40.572	40.611	40.651	40.690	40.729	40.768	40.807	40.846	40.885	980
990	40.885	40.924	40.963	41.002	41.042	41.081	41.120	41.159	41.198	41.237	41.276	990
1000	41.276	41.315	41.354	41.393	41.431	41.470	41.509	41.548	41.587	41.626	41.665	1000
1010	41.665	41.704	41.743	41.781	41.820	41.859	41.898	41.937	41.976	42.014	42.053	1010
1020	42.053	42.092	42.131	42.169	42.208	42.247	42.286	42.324	42.363	42.402	42.440	1020
1030	42.440	42.479	42.518	42.556	42.595	42.633	42.672	42.711	42.749	42.788	42.826	1030
1040	42.826	42.865	42.903	42.942	42.980	43.019	43.057	43.096	43.134	43.173	43.211	1040
1050	43.211	43.250	43.288	43.327	43.365	43.403	43.442	43.480	43.518	43.557	43.595	1050
1060	43.595	43.633	43.672	43.710	43.748	43.787	43.825	43.863	43.901	43.940	43.978	1060
1070	43.978	44.016	44.054	44.092	44.130	44.169	44.207	44.245	44.283	44.321	44.359	1070
1080	44.359	44.397	44.435	44.473	44.512	44.550	44.588	44.626	44.664	44.702	44.740	1080
1090	44.740	44.778	44.816	44.853	44.891	44.929	44.967	45.005	45.043	45.081	45.119	1090
°C	0	1	2	3	4	5	6	7	8	9	10	°C

°C	0	1	2	3	4	5	6	7	8	9	10	°C
1100	45.119	45.157	45.194	45.232	45.270	45.308	45.346	45.383	45.421	45.459	45.497	1100
1110	45.497	45.534	45.572	45.610	45.647	45.685	45.723	45.760	45.798	45.836	45.873	1110
1120	45.873	45.911	45.948	45.986	46.024	46.061	46.099	46.136	46.174	46.211	46.249	1120
1130	46.249	46.286	46.324	46.361	46.398	46.436	46.473	46.511	46.548	46.585	46.623	1130
1140	46.623	46.660	46.697	46.735	46.772	46.809	46.847	46.884	46.921	46.958	46.995	1140
1150	46.995	47.033	47.070	47.107	47.144	47.181	47.218	47.256	47.293	47.330	47.367	1150
1160	47.367	47.404	47.441	47.478	47.515	47.552	47.589	47.626	47.663	47.700	47.737	1160
1170	47.737	47.774	47.811	47.848	47.884	47.921	47.958	47.995	48.032	48.069	48.105	1170
1180	48.105	48.142	48.179	48.216	48.252	48.289	48.326	48.363	48.399	48.436	48.473	1180
1190	48.473	48.509	48.546	48.582	48.619	48.656	48.692	48.729	48.765	48.802	48.838	1190
1200	48.838	48.875	48.911	48.948	48.984	49.021	49.057	49.093	49.130	49.166	49.202	1200
1210	49.202	49.239	49.275	49.311	49.348	49.384	49.420	49.456	49.493	49.529	49.565	1210
1220	49.565	49.601	49.637	49.674	49.710	49.746	49.782	49.818	49.854	49.890	49.926	1220
1230	49.926	49.962	49.998	50.034	50.070	50.106	50.142	50.178	50.214	50.250	50.286	1230
1240	50.286	50.322	50.358	50.393	50.429	50.465	50.501	50.537	50.572	50.608	50.644	1240
1250	50.644	50.680	50.715	50.751	50.787	50.822	50.858	50.894	50.929	50.965	51.000	1250
1260	51.000	51.036	51.071	51.107	51.142	51.178	51.213	51.249	51.284	51.320	51.355	1260
1270	51.355	51.391	51.426	51.461	51.497	51.532	51.567	51.603	51.638	51.673	51.708	1270
1280	51.708	51.744	51.779	51.814	51.849	51.885	51.920	51.955	51.990	52.025	52.060	1280
1290	52.060	52.095	52.130	52.165	52.200	52.235	52.270	52.305	52.340	52.375	52.410	1290
1300	52.410	52.445	52.480	52.515	52.550	52.585	52.620	52.654	52.689	52.724	52.759	1300
1310	52.759	52.794	52.828	52.863	52.898	52.932	52.967	53.002	53.037	53.071	53.106	1310
1320	53.106	53.140	53.175	53.210	53.244	53.279	53.313	53.348	53.382	53.417	53.451	1320
1330	53.451	53.486	53.520	53.555	53.589	53.623	53.658	53.692	53.727	53.761	53.795	1330
1340	53.795	53.830	53.864	53.898	53.932	53.967	54.001	54.035	54.069	54.104	54.138	1340
1350	54.138	54.172	54.206	54.240	54.274	54.308	54.343	54.377	54.411	54.445	54.479	1350
1360	54.479	54.513	54.547	54.581	54.615	54.649	54.683	54.717	54.751	54.785	54.819	1360
1370	54.819	54.852	54.886									1370
°C	0	1	2	3	4	5	6	7	8	9	10	°C

MAXIMUM TEMPERATURE RANGE
Thermocouple Grade
– 328 to 2282°F
– 200 to 1250°C
Extension Grade
32 to 392°F
0 to 200°C
LIMITS OF ERROR
(whichever is greater)
Standard: 2.2°C or 0.75% Above 0°C
2.2°C or 2.0% Below 0°C
Special: 1.1°C or 0.4%
COMMENTS, BARE WIRE ENVIRONMENT:
Clean Oxidizing and Inert; Limited Use in Vacuum or Reducing; Wide Temperature Range; Most Popular Calibration
TEMPERATURE IN DEGREES °C
REFERENCE JUNCTION AT 0°C

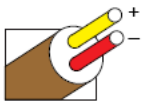

Thermocouple Grade

Nickel-Chromium
vs.
Nickel-Aluminum

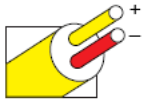

Extension Grade

Revised Thermocouple Reference Tables

TYPE K

Reference Tables
N.I.S.T. Monograph 175
Revised to ITS-90

Z

Thermoelectric Voltage in Millivolts

°C	-10	-9	-8	-7	-6	-5	-4	-3	-2	-1	0	°C
-260	-6.458	-6.457	-6.456	-6.455	-6.453	-6.452	-6.450	-6.448	-6.446	-6.444	-6.441	-260
-250	-6.441	-6.438	-6.435	-6.432	-6.429	-6.425	-6.421	-6.417	-6.413	-6.408	-6.404	-250
-240	-6.404	-6.399	-6.393	-6.388	-6.382	-6.377	-6.370	-6.364	-6.358	-6.351	-6.344	-240
-230	-6.344	-6.337	-6.329	-6.322	-6.314	-6.306	-6.297	-6.289	-6.280	-6.271	-6.262	-230
-220	-6.262	-6.252	-6.243	-6.233	-6.223	-6.213	-6.202	-6.192	-6.181	-6.170	-6.158	-220
-210	-6.158	-6.147	-6.135	-6.123	-6.111	-6.099	-6.087	-6.074	-6.061	-6.048	-6.035	-210
-200	-6.035	-6.021	-6.007	-5.994	-5.980	-5.965	-5.951	-5.936	-5.922	-5.907	-5.891	-200
-190	-5.891	-5.876	-5.861	-5.845	-5.829	-5.813	-5.797	-5.780	-5.763	-5.747	-5.730	-190
-180	-5.730	-5.713	-5.695	-5.678	-5.660	-5.642	-5.624	-5.606	-5.589	-5.569	-5.550	-180
-170	-5.550	-5.531	-5.512	-5.493	-5.474	-5.454	-5.435	-5.415	-5.395	-5.374	-5.354	-170
-160	-5.354	-5.333	-5.313	-5.292	-5.271	-5.250	-5.228	-5.207	-5.185	-5.163	-5.141	-160
-150	-5.141	-5.119	-5.097	-5.074	-5.052	-5.029	-5.006	-4.983	-4.960	-4.936	-4.913	-150
-140	-4.913	-4.889	-4.865	-4.841	-4.817	-4.793	-4.768	-4.744	-4.719	-4.694	-4.669	-140
-130	-4.669	-4.644	-4.618	-4.593	-4.567	-4.542	-4.516	-4.490	-4.463	-4.437	-4.411	-130
-120	-4.411	-4.384	-4.357	-4.330	-4.303	-4.276	-4.249	-4.221	-4.194	-4.166	-4.138	-120
-110	-4.138	-4.110	-4.082	-4.054	-4.025	-3.997	-3.968	-3.939	-3.911	-3.882	-3.852	-110
-100	-3.852	-3.823	-3.794	-3.764	-3.734	-3.705	-3.675	-3.645	-3.614	-3.584	-3.554	-100
-90	-3.554	-3.523	-3.492	-3.462	-3.431	-3.400	-3.368	-3.337	-3.306	-3.274	-3.243	-90
-80	-3.243	-3.211	-3.179	-3.147	-3.115	-3.083	-3.050	-3.018	-2.986	-2.953	-2.920	-80
-70	-2.920	-2.887	-2.854	-2.821	-2.788	-2.755	-2.721	-2.688	-2.654	-2.620	-2.587	-70
-60	-2.587	-2.553	-2.519	-2.485	-2.450	-2.416	-2.382	-2.347	-2.312	-2.278	-2.243	-60
-50	-2.243	-2.208	-2.173	-2.138	-2.103	-2.067	-2.032	-1.996	-1.961	-1.925	-1.889	-50
-40	-1.889	-1.854	-1.818	-1.782	-1.745	-1.709	-1.673	-1.637	-1.600	-1.564	-1.527	-40
-30	-1.527	-1.490	-1.453	-1.417	-1.380	-1.343	-1.305	-1.268	-1.231	-1.194	-1.156	-30
-20	-1.156	-1.119	-1.081	-1.043	-1.006	-0.968	-0.930	-0.892	-0.854	-0.816	-0.778	-20
-10	-0.778	-0.739	-0.701	-0.663	-0.624	-0.586	-0.547	-0.508	-0.470	-0.431	-0.392	-10
0	-0.392	-0.353	-0.314	-0.275	-0.236	-0.197	-0.157	-0.118	-0.079	-0.039	0.000	0
0	0.000	0.039	0.079	0.119	0.158	0.198	0.238	0.277	0.317	0.357	0.397	0
10	0.397	0.437	0.477	0.517	0.557	0.597	0.637	0.677	0.718	0.758	0.798	10
20	0.798	0.838	0.879	0.919	0.960	1.000	1.041	1.081	1.122	1.163	1.203	20
30	1.203	1.244	1.285	1.326	1.366	1.407	1.448	1.489	1.530	1.571	1.612	30
40	1.612	1.653	1.694	1.735	1.776	1.817	1.858	1.899	1.941	1.982	2.023	40
50	2.023	2.064	2.106	2.147	2.188	2.230	2.271	2.312	2.354	2.395	2.436	50
60	2.436	2.478	2.519	2.561	2.602	2.644	2.685	2.727	2.768	2.810	2.851	60
70	2.851	2.893	2.934	2.976	3.017	3.059	3.100	3.142	3.184	3.225	3.267	70
80	3.267	3.308	3.350	3.391	3.433	3.474	3.516	3.557	3.599	3.640	3.682	80
90	3.682	3.723	3.765	3.806	3.848	3.889	3.931	3.972	4.013	4.055	4.096	90
100	4.096	4.138	4.179	4.220	4.262	4.303	4.344	4.385	4.427	4.468	4.509	100
110	4.509	4.550	4.591	4.633	4.674	4.715	4.756	4.797	4.838	4.879	4.920	110
120	4.920	4.961	5.002	5.043	5.084	5.124	5.165	5.206	5.247	5.288	5.328	120
130	5.328	5.369	5.410	5.450	5.491	5.532	5.572	5.613	5.653	5.694	5.735	130
140	5.735	5.775	5.815	5.856	5.896	5.937	5.977	6.017	6.058	6.098	6.138	140
150	6.138	6.179	6.219	6.259	6.299	6.339	6.380	6.420	6.460	6.500	6.540	150
160	6.540	6.580	6.620	6.660	6.701	6.741	6.781	6.821	6.861	6.901	6.941	160
170	6.941	6.981	7.021	7.060	7.100	7.140	7.180	7.220	7.260	7.300	7.340	170
180	7.340	7.380	7.420	7.460	7.500	7.540	7.579	7.619	7.659	7.699	7.739	180
190	7.739	7.779	7.819	7.859	7.899	7.939	7.979	8.019	8.059	8.099	8.138	190
200	8.138	8.178	8.218	8.258	8.298	8.338	8.378	8.418	8.458	8.499	8.539	200
210	8.539	8.579	8.619	8.659	8.699	8.739	8.779	8.819	8.860	8.900	8.940	210
220	8.940	8.980	9.020	9.061	9.101	9.141	9.181	9.222	9.262	9.302	9.343	220
230	9.343	9.383	9.423	9.464	9.504	9.545	9.585	9.626	9.666	9.707	9.747	230
240	9.747	9.788	9.828	9.869	9.909	9.950	9.991	10.031	10.072	10.113	10.153	240
°C	0	1	2	3	4	5	6	7	8	9	10	°C

°C	0	1	2	3	4	5	6	7	8	9	10	°C
250	10.153	10.194	10.235	10.276	10.316	10.357	10.398	10.439	10.480	10.520	10.561	250
260	10.561	10.602	10.643	10.684	10.725	10.766	10.807	10.848	10.889	10.930	10.971	260
270	10.971	11.012	11.053	11.094	11.135	11.176	11.217	11.259	11.300	11.341	11.382	270
280	11.382	11.423	11.465	11.506	11.547	11.588	11.630	11.671	11.712	11.753	11.795	280
290	11.795	11.836	11.877	11.919	11.960	12.001	12.043	12.084	12.126	12.167	12.209	290
300	12.209	12.250	12.291	12.333	12.374	12.416	12.457	12.499	12.540	12.582	12.624	300
310	12.624	12.665	12.707	12.748	12.790	12.831	12.873	12.915	12.956	12.998	13.040	310
320	13.040	13.081	13.123	13.165	13.206	13.248	13.290	13.331	13.373	13.415	13.457	320
330	13.457	13.498	13.540	13.582	13.624	13.665	13.707	13.749	13.791	13.833	13.874	330
340	13.874	13.916	13.958	14.000	14.042	14.084	14.126	14.167	14.209	14.251	14.293	340
350	14.293	14.335	14.377	14.419	14.461	14.503	14.545	14.587	14.629	14.671	14.713	350
360	14.713	14.755	14.797	14.839	14.881	14.923	14.965	15.007	15.049	15.091	15.133	360
370	15.133	15.175	15.217	15.259	15.301	15.343	15.385	15.427	15.469	15.511	15.554	370
380	15.554	15.596	15.638	15.680	15.722	15.764	15.806	15.849	15.891	15.933	15.975	380
390	15.975	16.017	16.059	16.102	16.144	16.186	16.228	16.270	16.313	16.355	16.397	390
400	16.397	16.439	16.482	16.524	16.566	16.608	16.651	16.693	16.735	16.778	16.820	400
410	16.820	16.862	16.904	16.947	16.989	17.031	17.074	17.116	17.158	17.201	17.243	410
420	17.243	17.285	17.328	17.370	17.413	17.455	17.497	17.540	17.582	17.624	17.667	420
430	17.667	17.709	17.752	17.794	17.837	17.879	17.921	17.964	18.006	18.049	18.091	430
440	18.091	18.134	18.176	18.218	18.261	18.303	18.346	18.388	18.431	18.473	18.516	440
450	18.516	18.558	18.601	18.643	18.686	18.728	18.771	18.813	18.856	18.898	18.941	450
460	18.941	18.983	19.026	19.068	19.111	19.154	19.196	19.239	19.281	19.324	19.366	460
470	19.366	19.409	19.451	19.494	19.537	19.579	19.622	19.664	19.707	19.750	19.792	470
480	19.792	19.835	19.877	19.920	19.962	20.005	20.048	20.090	20.133	20.175	20.218	480
490	20.218	20.261	20.303	20.346	20.389	20.431	20.474	20.516	20.559	20.602	20.644	490
500	20.644	20.687	20.730	20.772	20.815	20.857	20.900	20.943	20.985	21.028	21.071	500
510	21.071	21.113	21.156	21.199	21.241	21.284	21.326	21.369	21.412	21.454	21.497	510
520	21.497	21.540	21.582	21.625	21.668	21.710	21.753	21.796	21.838	21.881	21.924	520
530	21.924	21.966	22.009	22.052	22.094	22.137	22.179	22.222	22.265	22.307	22.350	530
540	22.350	22.393	22.435	22.478	22.521	22.563	22.606	22.649	22.691	22.734	22.776	540
550	22.776	22.819	22.862	22.904	22.947	22.990	23.032	23.075	23.117	23.160	23.203	550
560	23.203	23.245	23.288	23.331	23.373	23.416	23.458	23.501	23.544	23.586	23.629	560
570	23.629	23.671	23.714	23.757	23.799	23.842	23.884	23.927	23.970	24.012	24.055	570
580	24.055	24.097	24.140	24.182	24.225	24.267	24.310	24.353	24.395	24.438	24.480	580
590	24.480	24.523	24.565	24.608	24.650	24.693	24.735	24.778	24.820	24.863	24.905	590
600	24.905	24.948	24.990	25.033	25.075	25.118	25.160	25.203	25.245	25.288	25.330	600
610	25.330	25.373	25.415	25.458	25.500	25.543	25.585	25.627	25.670	25.712	25.755	610
620	25.755	25.797	25.840	25.882	25.924	25.967	26.009	26.052	26.094	26.136	26.179	620
630	26.179	26.221	26.263	26.306	26.348	26.390	26.433	26.475	26.517	26.560	26.602	630
640	26.602	26.644	26.687	26.729	26.771	26.814	26.856	26.898	26.940	26.983	27.025	640
650	27.025	27.067	27.109	27.152	27.194	27.236	27.278	27.320	27.363	27.405	27.447	650
660	27.447	27.489	27.531	27.574	27.616	27.658	27.700	27.742	27.784	27.826	27.869	660
670	27.869	27.911	27.953	27.995	28.037	28.079	28.121	28.163	28.205	28.247	28.289	670
680	28.289	28.332	28.374	28.416	28.458	28.500	28.542	28.584	28.626	28.668	28.710	680
690	28.710	28.752	28.794	28.835	28.877	28.919	28.961	29.003	29.045	29.087	29.129	690
700	29.129	29.171	29.213	29.255	29.297	29.338	29.380	29.422	29.464	29.506	29.548	700
710	29.548	29.589	29.631	29.673	29.715	29.757	29.798	29.840	29.882	29.924	29.965	710
720	29.965	30.007	30.049	30.090	30.132	30.174	30.216	30.257	30.299	30.341	30.382	720
730	30.382	30.424	30.466	30.507	30.549	30.590	30.632	30.674	30.715	30.757	30.798	730
740	30.798	30.840	30.881	30.923	30.964	31.006	31.047	31.089	31.130	31.172	31.213	740
750	31.213	31.255	31.296	31.338	31.379	31.421	31.462	31.504	31.545	31.586	31.628	750
760	31.628	31.669	31.710	31.752	31.793	31.834	31.876	31.917	31.958	32.000	32.041	760
770	32.041	32.082	32.124	32.165	32.206	32.247	32.289	32.330	32.371	32.412	32.453	770
780	32.453	32.495	32.536	32.577	32.618	32.659	32.700	32.742	32.783	32.824	32.865	780
790	32.865	32.906	32.947	32.988	33.029	33.070	33.111	33.152	33.193	33.234	33.275	790
°C	0	1	2	3	4	5	6	7	8	9	10	°C

Z-204

From [13].

Appendix D

LDA and CARS Measurements

DJHC-I

r (mm)	v (m/s)
-40	1,0401
-35	3,4487
-30	4,3779
-25	4,5365
-20	4,1947
-15	3,6665
-10	3,04
-8	2,645
-6	2,2156
-5	1,9475
-4	1,7551
-3	1,5656
0	34,05
3	1,6167
4	1,9257
6	2,4007
8	2,7919
10	3,1512
15	4,0036
20	4,4947
25	4,55
30	4,3382
35	3,6511
40	1,1593

DJHC-X

r (mm)	v (m/s)
-40	1,0109
-35	3,3686
-30	4,2346
-25	4,4466
-20	4,0803
-15	3,5997
-10	2,9532
-8	2,6262
-6	2,2332
-5	1,9943
-4	1,771
-3	1,5707
0	32,858
3	1,7394
4	2,0306
5	2,3263
6	2,5239
8	2,8547
10	3,234
15	3,9798
20	4,3894
25	4,4272
30	4,1526
35	3,3246
40	0,87772

Figure D.1: Velocity-data as measured with LDA at a distance $3\,\mathrm{mm}$ from the top of the fuel-duct, for coflow I and coflow X. Only the velocities above the annulus, from $r = -35\,\mathrm{mm}$ to $r = -4\,\mathrm{mm}$ and from $r = 4\,\mathrm{mm}$ to $r = 35\,\mathrm{mm}$, have been used for calculations. [12]

DJHC-I

r (mm)	T (K)	h (J/g)
-35	1229	1409,20
-30	1422	1661,71
-25	1538	1816,33
-22	1562	1848,72
-20	1564	1851,62
-18	1549	1831,07
-16	1524	1797,57
-14	1466	1720,15
-12	1410	1645,85
-10	1336	1548,40
-8	1249	1435,05
-6	1189	1357,72
-5	1135	1288,64
-4	1086	1226,52
-3	967	
-2	644	
-1	510	
0	470	
1	477	
2	601	
3	958	
4	1143	1298,82
5	1208	1382,13
6	1277	1471,38
8	1371	1594,41
10	1420	1659,06
12	1448	1696,21
14	1533	1809,63
16	1544	1824,37
18	1552	1835,09
20	1546	1827,05
22	1563	1850,17
25	1532	1808,29
30	1444	1690,90
35	1265	1455,79

DJHC-X

r (mm)	T (K)	h (J/g)
-35	1020	1131,27
-30	1172	1320,78
-25		1428,69
-22	1377	1583,25
-20	1390	1600,14
-18	1389	1598,84
-16	1365	1567,70
-14	1328	1519,83
-12	1284	1463,25
-10	1236	1401,92
-8	1197	1352,40
-6	1108	1240,38
-5	1066	1188,10
-4	1013	1122,68
-3	906	
-2	536	
-1	488	
0	477	
1	484	
2	568	
3	891	
4	996	1101,83
5	1062	1183,14
6	1116	1250,38
8	1187	1339,75
10	1248	1417,21
12	1295	1477,37
14	1343	1539,21
16	1369	1572,88
18	1400	1613,13
20	1410	1626,14
22	1403	1617,03
25	1378	1584,55
30	1298	1481,21
35	1160	1305,61

Figure D.2: Temperature-data as measured with CARS at a distance $3\,\mathrm{mm}$ from the top of the fuel-duct, for coflow I and coflow X. Included are the (temperature-related) enthalpies, found by linear interpolation of the data in Appendix B. Only the measurements above the annulus, from $r = -35\,\mathrm{mm}$ to $r = -4\,\mathrm{mm}$ and from $r = 4\,\mathrm{mm}$ to $r = 35\,\mathrm{mm}$, have been used for calculations. [12]

Appendix E

Polynomials Fits to LDA and CARS Data

Using *Microsoft Excel* and the data from Appendix D, fourth-order polynomial fits were constructed for the velocity v, temperature T and enthalpy h.

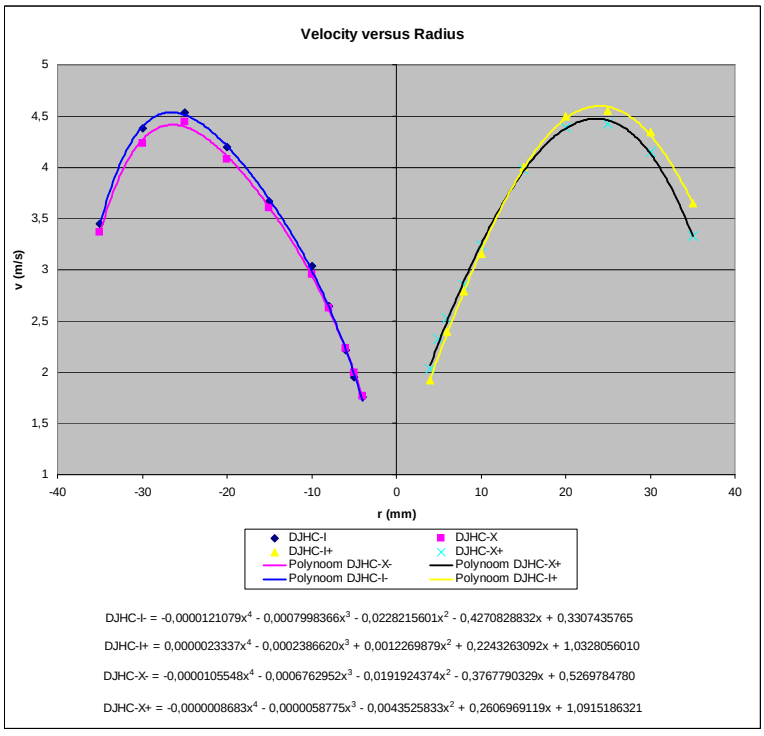

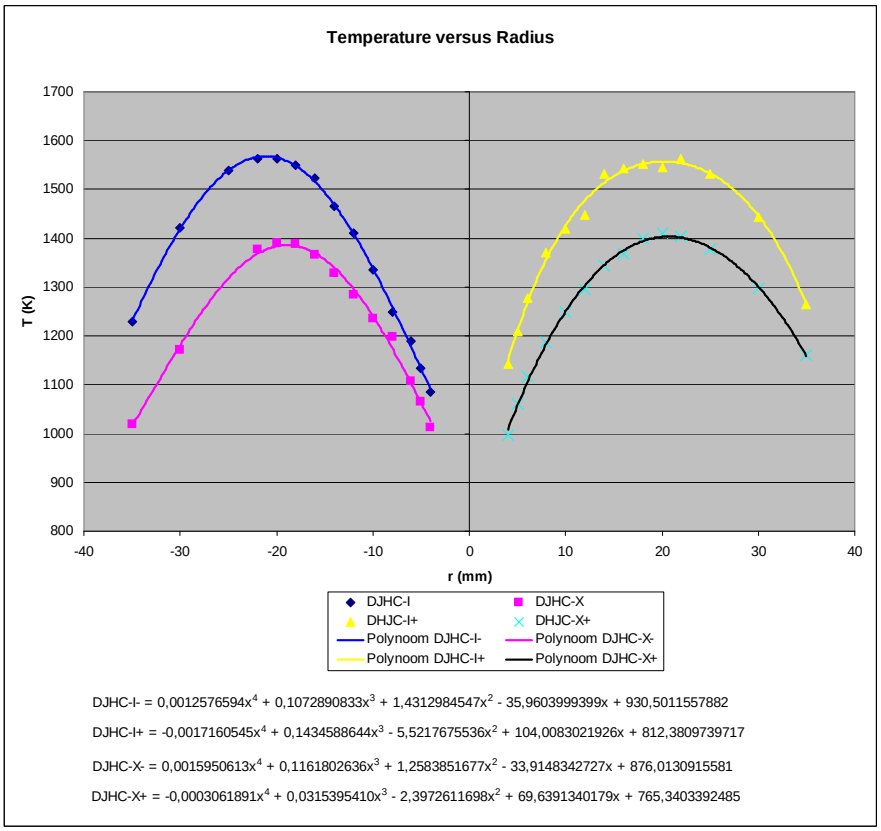

DJHC-I- = $0{,}0012576594x^4 + 0{,}1072890833x^3 + 1{,}4312984547x^2 - 35{,}9603999399x + 930{,}5011557882$

DJHC-I+ = $-0{,}0017160545x^4 + 0{,}1434588644x^3 - 5{,}5217675536x^2 + 104{,}0083021926x + 812{,}3809739717$

DJHC-X- = $0{,}0015950613x^4 + 0{,}1161802636x^3 + 1{,}2583851677x^2 - 33{,}9148342727x + 876{,}0130915581$

DJHC-X+ = $-0{,}0003061891x^4 + 0{,}0315395410x^3 - 2{,}3972611698x^2 + 69{,}6391340179x + 765{,}3403392485$

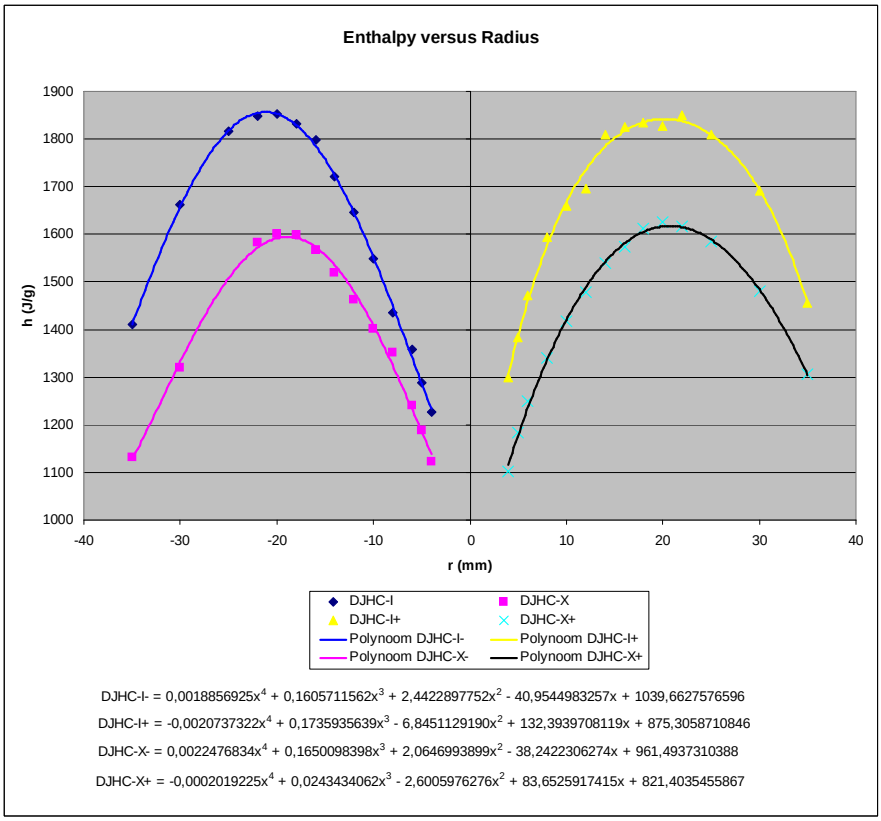

$DJHC\text{-}I- = 0{,}0018856925x^4 + 0{,}1605711562x^3 + 2{,}4422897752x^2 - 40{,}9544983257x + 1039{,}6627576596$

$DJHC\text{-}I+ = -0{,}0020737322x^4 + 0{,}1735935639x^3 - 6{,}8451129190x^2 + 132{,}3939708119x + 875{,}3058710846$

$DJHC\text{-}X- = 0{,}0022476834x^4 + 0{,}1650098398x^3 + 2{,}0646993899x^2 - 38{,}2422306274x + 961{,}4937310388$

$DJHC\text{-}X+ = -0{,}0002019225x^4 + 0{,}0243434062x^3 - 2{,}6005976276x^2 + 83{,}6525917415x + 821{,}4035455867$

Appendix F

Wall Temperature Measurements

		TC1	TC2	TC3	TC4	TC5
	z(m)	**0,5**	**0,4**	**0,3**	**0,2**	**0,1**
I-a	**U (mV)**	9,40	13,60	15,80	18,30	17,50
	Ucorr (mV)	9,38	13,57	15,76	18,26	17,46
	T (C)	231	333	385	444	425
	T (K)	**504**	**606**	**658**	**717**	**698**
I-b	**U (mV)**	9,24	13,61	16,42	20,15	18,25
	Ucorr (mV)	9,22	13,58	16,38	20,10	18,21
	T (C)	227	333	400	487	443
	T (K)	**500**	**606**	**673**	**760**	**716**
X-a	**U (mV)**	9,00	12,40	13,10	16,00	15,80
	Ucorr (mV)	8,98	12,37	13,07	15,96	15,76
	T (C)	221	304	321	390	385
	T (K)	**494**	**577**	**594**	**663**	**658**
X-b	**U (mV)**	8,76	12,29	14,34	17,72	16,49
	Ucorr (mV)	8,74	12,26	14,31	17,68	16,45
	T (C)	215	301	350	430	401
	T (K)	**488**	**574**	**623**	**703**	**674**

Figure F.1: Measured thermocouple voltages U at height z, the corrected voltage U_{corr} and corresponding temperatures T for mixtures I and X. Both have been measured twice, at two different times (a and b).